

A Social Context-aware Graph-based Multimodal Attentive Learning Framework for Disaster Content Classification during Emergencies

Shahid Shafi Dar^{a,*}, Mohammad Zia Ur Rehman^a, Karan Bais^b, Mohammed Abdul Haseeb^c and Nagendra Kumar^a

^aIndian Institute of Technology Indore, 453552, India

^bInstitute of Engineering and Technology, Devi Ahilya Vishwavidyalaya, 452017, India

^cIndian Institute of Information Technology Dharwad, 580009, India

ARTICLE INFO

Keywords:

Disaster Content Classification

Deep Learning

Crisis Management

Multimodal Data

Data Fusion

Abstract

In times of crisis, the prompt and precise classification of disaster-related information shared on social media platforms is of paramount importance for effective disaster response and public safety. During such critical events, people utilize social media as a medium for communication, sharing multimodal textual and visual content. However, due to the substantial influx of unfiltered and diverse data, humanitarian organizations face challenges in effectively leveraging this information. Numerous methods have been proposed for classifying disaster-related content, but these methods lack modeling users' credibility, emotional context, and social interaction information, which is crucial for classification. In this context, we propose a method, CrisisSpot, that leverages a Graph-based Neural Network to comprehend intricate relationships between textual and visual modalities and Social Context Features to incorporate user-centric and content-centric information. We also propose Inverted Dual Embedded Attention, which captures both harmonious and contrary patterns present in the data to harness complex interactions and facilitate richer insights in multimodal data. We have developed a multimodal disaster dataset, TSEqD (Turkey-Syria Earthquake Dataset), which is a large annotated dataset for a single disaster event containing 10,352 data samples. Through extensive experimentation, CrisisSpot has demonstrated significant improvements, achieving an average gain of 9.45% and 5.01% in F1-score compared to the state-of-the-art methods on the publicly available CrisisMMD dataset and TSEqD dataset, respectively.

1. Introduction

The rising frequency and growing severity of natural disasters, such as earthquakes, floods, and hurricanes, cause a significant socio-economic disturbance on a global scale [1]. These events have a devastating impact on the economy, human health, and livelihood. In 2022 alone, there were 387 natural disasters, resulting in 30,704 deaths and affecting approximately 185 million people, causing millions of dollars of damage costs as reported by the Emergency Event Database (EM-DAT)¹. In addition to physical damages, these disasters often lead to homelessness, mental health issues, unemployment, emotional distress, financial difficulties, and economic recession. Therefore, it is crucial to consistently explore innovative and enhanced approaches for response and recovery during disasters.

Role of Social Media during Disaster Events

Social media platforms have emerged as invaluable real-time information sources during disaster events [2]. These platforms serve as channels for the rapid dissemination of information, providing critical real-time updates and firsthand accounts during such events [3, 4]. For instance, during the 2023 Turkey-Syria earthquake, social media² served as an

*Corresponding author

✉ phd2201201004@iiti.ac.in (S.S. Dar); phd2101201005@iiti.ac.in (M.Z.U. Rehman); karanbais2701@gmail.com (K. Bais); 20bcs085@iiitdwd.ac.in (M.A. Haseeb); nagendra@iiti.ac.in (N. Kumar)

¹<https://reliefweb.int/report/world/2022-disasters-numbers>

²<https://news.northeastern.edu/2023/02/08/social-media-turkey-earthquake/>

indispensable communication platform, facilitating rescue requests and streamlining the coordination of aid efforts. Numerous individuals who were stuck beneath debris utilized mobile tools to access social media platforms, seeking rescue assistance by sharing messages on social media³, which signifies the utility of social media during such events. However, the research community faces numerous challenges in utilizing social media information during crisis events.

Challenges in Leveraging Social Media Information

The real-time information provided by social media platforms enhances crisis management capabilities [5], but the overwhelming influx of irrelevant data delays disaster response and management [6] as manual segregation of the relevant information is a time-consuming and costly process. Identifying relevant content amidst this digital noise is a significant challenge. Another important aspect is the incorporation of a diverse mixture of multimodal data [7, 8], encompassing images and text. Each of these modalities presents its own complexities. For instance, the text in crisis-related social media posts often uses informal language, contains frequent misspellings, incorporates numerous hashtags, and mentions other users. Relying solely on text analysis may not capture the full context of a situation [9]. Conversely, images, when viewed in isolation, may lack the necessary context for effective decision-making. To this end, we propose CrisisSpot, a robust and versatile disaster content classification method. The proposed approach merges linguistic context with visual evidence to create a more comprehensive understanding of disaster situations. A system like CrisisSpot empowers stakeholders by allowing them to effectively classify and respond to the most pertinent information contained within social media data posted during a disaster.

Existing Multimodal Paradigms and Limitations

It is worth noting that previous works [9–13] have often overlooked the utilization of Social Context Features (SCF). SCF [14] is an umbrella term that consists of social interaction metrics and semantic text information. They provide a multifaceted view of disaster-related content by incorporating factors such as the credibility of information [15], emotional context [16], and user engagement. In the existing works, various approaches have been proposed over time [9, 12, 13, 17–19]. Alam *et al.* [13] utilize the K-nearest neighbor method for constructing a nearest-neighbor graph. In their methodology, nodes are updated based on intra-cluster information, while CrisisSpot updates nodes using neighborhood information selected from the entire dataset across multiple iterations. Consequently, CrisisSpot provides a comprehensive overview of data to each node for feature refinement. Additionally, their choice of neighborhood based on Euclidean distance between nodes is suboptimal for high-dimensional data spaces [20]. To this end, CrisisSpot employs cosine similarity for neighbor selection, a metric proven to perform better in high-dimensional spaces.

Abavisani *et al.* [18] utilize SSE-Graph [21], which relies on the knowledge graph for swapping embeddings, but it may not explicitly capture the complex structural relationships within the graph. Also, depending on the size of the knowledge graph and the frequency of swapping, SSE-Graph may face scalability challenges. Handling large-scale graphs with frequent embedding swaps might lead to increased computational complexity. To this end, CrisisSpot excels at learning representations that capture the local graph topology, which can be crucial for certain tasks. Additionally, our graph-based approach is designed for scalable graph learning and may provide more efficient solutions for large graphs [22].

The aforementioned studies [9, 12, 18] employ conventional attention mechanisms such as cross-attention to focus solely on aligned information. In contrast, our proposed attention mechanism, Inverted Dual Embedded Attention (IDEA), adeptly directs attention to both aligned and misaligned information patterns across diverse modalities. This explicit recognition significantly augments the model's capability to effectively handle multimodal data. In conclusion, while existing multimodal paradigms have made significant strides, our study highlights some important research gaps. Our work addresses these limitations by integrating multimodal features, acknowledging the importance of Social Context Features (SCF), and introducing the Inverted Dual Embedded Attention (IDEA) mechanism.

Addressing Research Gaps: Our Solution at a Glance

In response to these gaps in the existing literature, our work introduces a novel approach based on the multimodal attentive framework for disaster content classification. Our approach serves a dual purpose: first, we classify data into informative and non-informative content. Subsequently, we classify the informative content into various humanitarian categories. To achieve this, we employ a graph-based approach that leverages intricate relationships among disaster-related content, enriching the model's contextual understanding. This graphical representation significantly enhances

³<https://www.theguardian.com/world/video/2023/feb/07/turkey-earthquake-victim-rescued-after-social-media-plea-under-rubble-video>

our model's ability to discern subtle nuances within crisis-related information. Furthermore, we propose an attention mechanism tailored to identify both similar and dissimilar content pairs, thereby fostering a more nuanced comprehension of context. In addition to these advancements, our framework integrates Social Context Features, effectively utilizing text-centric and user-centric information. SCF, in our work, comprises User Informative Score (UIS), Crisis Informative Score (CIS), and User Engagement metrics. The UIS of SCF is of paramount importance in evaluating the user credibility of social media content. Similarly, the CIS of SCF measures the presence of crisis-related vocabulary in text, indicating a higher degree of informative content related to the crisis. It quantifies the semantic attributes of text. These features have often been neglected in previous works focused on disaster content classification.

In summary, our research presents a comprehensive and innovative approach to disaster content classification during emergencies. By harnessing the power of multimodal data, graph-based enriched context modeling, and Social Context Features, our framework equips emergency responders and humanitarian organizations with a more accurate and context-aware model.

Key Contributions

The key contributions of this work are outlined as follows:

1. We propose a “multimodal attentive learning framework” for the problem of disaster content classification for various crisis events. The proposed method leverages graph-based and attention-based approaches for feature enrichment and more nuanced comprehension of the model's prediction ability.
2. To the best of our knowledge, we are the first to leverage the potential of Social Context Features (SCF) for disaster content classification in multimodal settings. SCF, effectively merging text-centric and user-centric information, elevates model performance by considering content within a broader context encompassing user history, social interactions, and user credibility.
3. We propose an attention mechanism, Inverted Dual Embedded Attention (IDEA), which captures both harmonious and contrary information present in the modalities. IDEA enables CrisisSpot to capture dependencies and complex relationships within the data, leading to more robust feature representations and richer comprehension of multimodal content.
4. We have created a new dataset, TSEqD (Turkey-Syria Earthquake Dataset), which is a multimodal crisis dataset composed of 10,352 data samples. To the best of our knowledge, this is the largest single-event multimodal dataset annotated for both Informative and Humanitarian Tasks.
5. We have curated a list of 4,268 crisis-related lexicons, which are utilized to compute CIS, an important component of SCF. This comprehensive lexicon list may help researchers and humanitarian organizations efficiently assess and categorize disaster-related textual content.
6. We conduct comprehensive experiments on two data-sets, such as CrisisMMD and TSEqD, to evaluate the effectiveness of our proposed approach. The experimental outcomes clearly indicate that our approach surpasses state-of-the-art methods.

The subsequent sections of this article are organized as follows: In [Section 2](#), we provide a comprehensive review of the relevant literature. [Section 3](#) outlines our methodology, while [Section 4](#) presents the outcomes of our experimental assessments. Lastly, in [Section 5](#), we provide our concluding remarks on this study.

2. Related Work

We examine previous research on disaster content classification, categorizing these studies into two primary groups: unimodal and multimodal disaster content classification.

2.1. Unimodal Disaster Content Classification

Unimodal disaster content classification involves the process of classifying disaster-related content using a single data modality, which includes text and images. Two prevalent instances of unimodal disaster content classification are disaster text classification and disaster image classification.

2.1.1. Disaster Text Classification

Most of the previous research [23] on classifying disaster-related content has primarily concentrated on the textual modality. For instance, Ghafarian *et al.* [24] propose a method to identify informative tweets, leveraging the assumption that each tweet represents a word distribution. They performed experiments on 20 crisis incidents of various types. Rudra *et al.* [25] employed vocabulary-agnostic features, including syntactic features and basic lexical elements, to classify tweets as either conveying situational or non-situational information. They conducted experiments using various disaster datasets and compared their approach with the Bag-Of-Words (BOW) model for Hindi and English tweets. Kumar *et al.* [26] evaluated multiple traditional Machine Learning and advanced Deep Learning algorithms for categorizing tweets related to disasters across six distinct classes. The effectiveness of the models was assessed through testing on four specific disaster scenarios, such as wildfires, earthquakes, hurricanes, and floods. Xie *et al.* [27] uses a supervised contrastive learning technique for text classification for humanitarian content in social media. They conducted experiments on three distinct datasets, demonstrating that their method led to enhanced classification accuracy for the model. Nevertheless, prior approaches have made significant strides in addressing challenges associated with disaster text classification. However, they fail to address issues inherent to textual data, including non-standard English, spelling and grammatical errors, and unconventional abbreviations. Additionally, these methods neglect crucial informative factors, such as user credibility, user engagement data, and the emotional context within the text. These factors play a vital role in enhancing the model's classification capabilities, enabling it to identify relevant, reliable, and information-rich content within the text.

2.1.2. Disaster Image Classification

Due to the limited number of disaster image datasets, the predominant focus has shifted towards the development of comprehensive and high-quality image datasets [28, 29] within the field of disaster management. Most of the research focuses on categorizing the images based on the severity of the damage. Chaudhuri *et al.* [30] collect geotagged images from regions impacted by earthquakes. They apply a deep learning method to categorize these images, with a specific focus on identifying survivors under the rubble. They find that the deep learning method exhibits improved accuracy in image classification compared to conventional machine learning techniques. Nguyen *et al.* [31] employs a deep CNN to classify disaster-related images into various categories, such as severe, mild, and no-damage classes. Their CNN-based approach surpassed Bag-of-Visual-Words (BoVW) methods, achieving significant F1-scores between 0.67 and 0.89. Alam *et al.* [32] conducted image classification of disaster-related images sourced from social media to assess the extent of the damage. Their work underscored the significance of domain-specific fine-tuning of deep Convolutional Neural Networks. However, prior methods have made substantial progress in tackling the issues related to classifying disaster images. However, they fail to address issues inherent to image data, such as variations in data quality and the context-dependent nature of interpretation. These elements significantly contribute to augmenting the model's capabilities in classifying images.

2.2. Multimodal Disaster Content Classification

In recent times, researchers have introduced multimodal systems that harness both text and images to extract relevant information. Agarwal *et al.* [33] uses the CrisisMMD dataset [34] to build a multimodal end-to-end gated system that identifies the infrastructural damage cues in the data and further qualifies the damage severity of the data based on the ordinal quantification given in the dataset. They surpass state-of-the-art methods, by a significant amount. Abavisani *et al.* [18] proposed a new cross-attention module during the data fusion process to avoid propagating of false information. Koshy *et al.* [35] have introduced an advanced deep learning framework that integrates various input modalities, incorporating text and images derived from user-generated content. Their approach outlines a systematic methodology for distinguishing informative tweets from the vast volume of user-generated content on social media platforms. Madichetty *et al.* [36] have presented a novel technique for identifying informative tweets with multimodal content during disaster situations. Their method involves the utilization of pre-trained RoBERTa for text features and VGG-16 for image features. To combine these two model outputs, they employ a multiplicative fusion technique. However, prior multimodal methods have made significant progress in handling the issues related to disaster content classification. However, most of the prior methods did not incorporate graph-based learning techniques, which helps us enrich the features. Additionally, they overlooked various social interaction information, which enhances the classification abilities of the model.

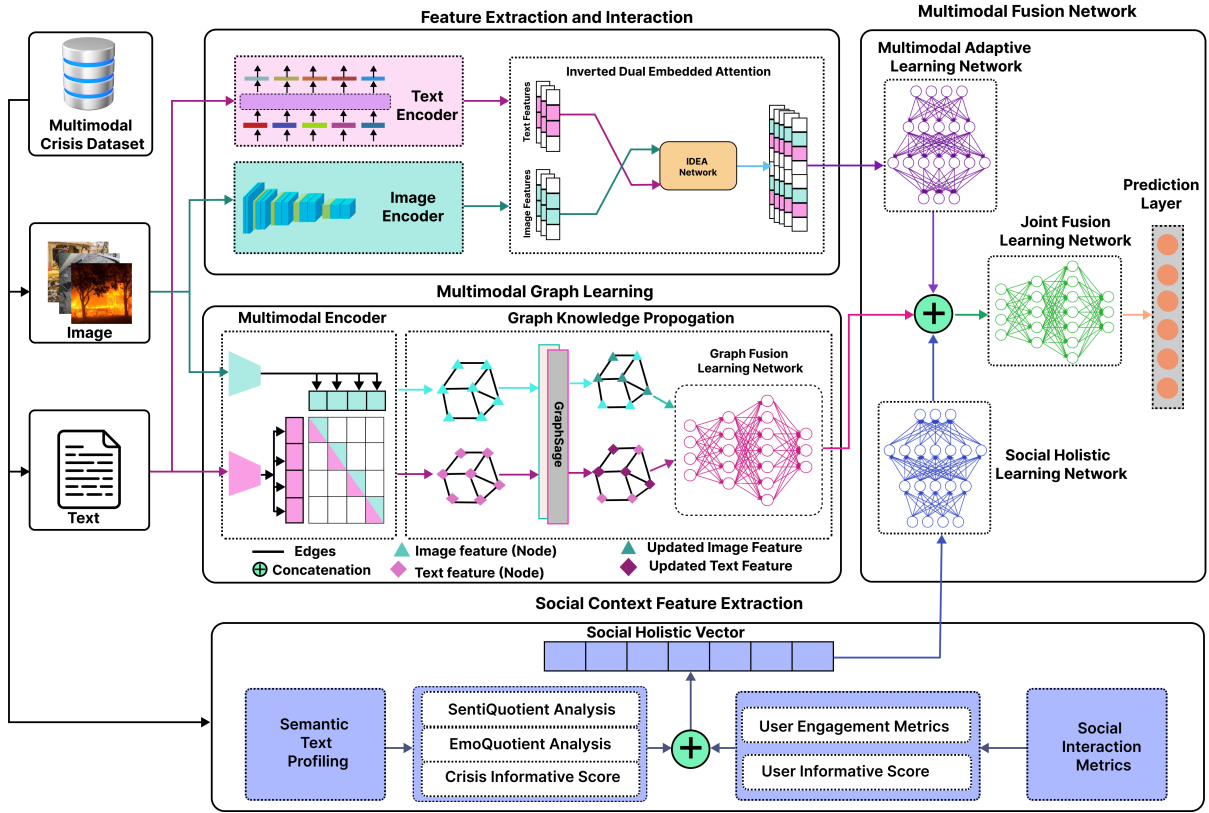


Figure 1: System Architecture of CrisisSpot. The features get updated after applying the GraphSAGE layer. The updated node features are depicted using a color representation that corresponds with darker shades.

3. Methodology

We present our proposed method by presenting its comprehensive description along with the overall architectural framework, as depicted in Fig. 1. The proposed methodology can be divided into four sub-modules, namely, Feature Extraction and Interaction, Multimodal Graph Learning, Social Context Feature Extraction, and Multimodal Fusion Network. Feature Extraction and Interaction focuses on extracting relevant features from text and visual modalities and capturing interactions via the multimodal attention mechanism (Inverted Dual Embedded Attention). Multimodal Graph Learning involves leveraging multimodal graph knowledge propagation to integrate information from text and image modalities. Social Context Feature Extraction concentrates on incorporating social interaction and text-based information into the model, enriching the model's context comprehension by incorporating valuable information from text-centric evaluations and user-oriented assessments. Multimodal Fusion Network encompasses the fusion of multimodal representations of data from all the modules, yielding a comprehensive output followed by a prediction layer to generate crisis predictions.

3.1. Feature Extraction and Interaction

In this section, we present a discussion about feature extraction and interaction processes. This module comprises two submodules: (a) Textual and Visual Feature Extraction and (b) Inverted Dual Embedded Attention.

3.1.1. Textual Feature Extraction

Each input modality is subjected to an initial encoding process, generating separate unimodal representations labeled as H_t for the textual modality and H_v for the visual modality. In the context of text modality, given a sequence of text tokens denoted as $S_t = \{T_1, T_2, T_3, \dots, T_n\}$, we employ the BERT-based [37] tokenization process to extract token

embeddings, resulting in the matrix H_t expressed in the following equation.

$$H_t = BERT(S_t) \in \mathbb{R}^{d \times dt} \quad (1)$$

In Eq. (1), H_t represents a matrix containing token embeddings, where $\mathbb{R}^{d \times dt}$ denotes a matrix with dimensions (d, dt) . We extract word-level features from the text encoder with a maximum sequence length of 128 and an embedding dimension of 768.

3.1.2. Visual Feature Extraction

The feature extraction process involves the utilization of the ResNet50 architecture, selectively extracting features up to the ‘conv4_block6_3_conv’ layer. The intention behind this decision is to capture complex and abstract representations that reside in deeper layers of the network. This is additionally performed to ensure that the shapes align with those of the text encoder, facilitating the interaction of features through the IDEA attention mechanism. The residual connections in ResNet50 facilitate effective gradient flow during training, addressing the vanishing gradient problem. The resulting feature map (F_{emb}) encapsulates hierarchical information, ranging from fundamental attributes such as edges and textures to more complex features such as object components and scenes. A bespoke convolutional layer, denoted as ‘custom_conv’, is seamlessly integrated into the architecture. This custom convolutional layer introduces 1024 filters and employs a (4, 4) kernel, inducing a transformative effect on the output shape, resulting in dimensions (11, 11, 1024). Subsequently, a crucial reshaping operation is applied to the feature map, yielding a tensor with dimensions (1, 121, 1024). This reshaping is strategically aligned with the subsequent processing requirements, ensuring optimal compatibility with the changing tensor structure. Simultaneously, a padding operation is introduced to the tensor to retain spatial information and maintain dimensional consistency. This step results in a tensor shape of (1, 128, 1024), crucial for the seamless progression of information through the network architecture. To safeguard the knowledge encoded in the ResNet50 pre-trained weights and fine-tune the model for the specialized image processing task, a discerning decision is made to freeze all original layers. This strategic freezing confines the training scope exclusively to the parameters of the ‘custom_conv’ layer. Equation (2) details the calculation of each element in the final visual feature matrix H_v , where the variable i represents the index of the features in the final visual feature matrix H_v . H_{img} and W_{img} represent the height and width of the feature map, respectively, and k denotes a specific channel within F_{emb} .

$$(H_v)_i = \frac{1}{H_{img} \cdot W_{img}} \sum_{w=1}^{W_{img}} \sum_{h=1}^{H_{img}} F_{emb}(h, w, k) \quad (2)$$

The sequence of changes in the architecture, involving adjustments in feature extraction, custom convolutional layer integration, reshaping, and padding, results in a customized ResNet model. This tailored adaptation enhances the model’s effectiveness for a specific image-processing application while leveraging the foundational knowledge inherent in the pre-trained ResNet-50 architecture.

3.1.3. Inverted Dual Embedded Attention (IDEA)

In multimodal data analysis, we often face the challenge of efficiently integrating information from various modalities, such as text and image, to achieve a holistic comprehension of the underlying content. Traditional attention mechanisms focus on aggregating information from multiple sources in which the modalities are aligned. However, they don’t focus on the contrary information present in the modalities. We propose an approach that recognizes both harmonious and contrary information present in the different modalities. The contrary information present between the modalities should be identified for several reasons. Contrary pairs highlight differences and inconsistencies between modalities. They contribute to enhanced model interpretability and provide insights into why a model makes specific decisions. They are crucial for tackling problems with noisy or misaligned multimodal data, ensuring a stronger and more dependable analysis. In this context, we introduce an attention mechanism called Inverted Dual Embedded Attention (IDEA). It combines harmonious and contrary attention vectors to reveal the complex interactions between different types of data. This unique strategy not only enhances the interpretability of the model but also provides a deeper understanding of multimodal information. By considering both harmonious and contrary attention, IDEA adapts to varying information needs, facilitating richer insights, improved representational learning, and a versatile approach

to multimodal data analysis. IDEA contains four modules: (a) Shared Embedding Module; (b) Harmonious Attention Module; (c) Contrary Attention Module; and (d) Attended Fusion Module.

3.1.3.1. Shared Embedding Module: In the shared embedding module. We take both the textual and visual features in the same embedding space, say $d_e=1024$. Projecting textual and visual modalities into a shared embedding space offers several key advantages in a multimodal setting, such as seamless integration of information from text and images, effective cross-modal attention, enabling semantic alignment, and parameter sharing, which reduces model complexity, leading to more efficient training and improved generalization. Two types of modality transformation occur here: textual modality transformation and visual modality transformation.

3.1.3.1.1. Textual Modality Transformation: In the initial stage, textual features $H_t \in \mathbb{R}^{d \times d_t}$ undergo a non-linear projection into a shared embedding space. This involves a linear transformation using trainable parameters $W_t \in \mathbb{R}^{d_t \times d_{se}}$ and $b_t \in \mathbb{R}^{1 \times d_{se}}$, resulting in $H_t W_t + b_t$ as the linearly projected textual features within the shared embedding space. The linearly projected textual features are subjected to a non-linear transformation denoted as $H_{Text} \in \mathbb{R}^{d \times d_{se}}$ that includes batch normalization [38, 39] and a hyperbolic tangent activation. Batch normalization helps in stabilizing and accelerating the training of deep neural networks by normalizing the inputs to each layer, reducing internal covariate shifts, and accelerating the training of deep neural networks. It normalizes the input of a layer by adjusting and scaling the activations. This can be shown in Eq. (3):

$$H_{Text} = \tanh \left(\gamma \odot \left(\frac{(H_t W_t + b_t) - \mu}{\sqrt{\sigma^2 + \epsilon}} \right) + \beta \right) \quad (3)$$

where γ and β are learnable parameters responsible for scaling and shifting, and μ and σ represent the mean and standard deviation calculated over the mini-batch of the input data, respectively. ϵ is a small constant added to the denominator in mathematical expressions to prevent division by zero or near-zero values, ensuring numerical stability. However, most of the deep learning frameworks, such as TensorFlow or PyTorch, have built-in functions for batch normalization. During training, these frameworks automatically calculate and update the mean and standard deviation over the mini-batches.

3.1.3.1.2. Visual Modality Transformation: This process is similar to that of textual modality. The only difference here is the transformation of the visual modality rather than the textual modality. In the initial stage, visual features $H_v \in \mathbb{R}^{d \times d_v}$ undergo a non-linear projection into a shared embedding space. This involves a linear transformation using trainable parameters $W_v \in \mathbb{R}^{d_v \times d_{se}}$ and $b_v \in \mathbb{R}^{1 \times d_{se}}$, resulting in $H_v W_v + b_v$ as the linearly projected visual features within the shared embedding space.

The linearly projected visual features are subjected to a non-linear transformation denoted as $H_{Vis} \in \mathbb{R}^{d \times d_{se}}$ that includes batch normalization [38, 39] and a hyperbolic tangent activation as expressed by the Eq. (4):

$$H_{Vis} = \tanh \left(\gamma \odot \left(\frac{(H_v W_v + b_v) - \mu}{\sqrt{\sigma^2 + \epsilon}} \right) + \beta \right) \quad (4)$$

where γ , β , μ and σ are already defined in Eq. (3) The dimensions of various parameters in our case are $d = 128$, $d_{se} = 1024$, $d_t = 768$, and $d_v = 1024$.

3.1.3.1.3. Similarity Matrix Computation: To compute the similarity matrix $S_{sim}[i, j] \in \mathbb{R}^{d \times d}$, we first compute $\hat{S}_{sim}[i, k] \in \mathbb{R}^{d \times d_{se}}$ by applying the element-wise tangent hyperbolic (tanh) function to the sum of the projected textual feature vectors $H_{Text}[i, m] \in \mathbb{R}^{d \times d_{se}}$ and visual feature vectors $H_{Vis}[i, m] \in \mathbb{R}^{d \times d_{se}}$ as shown in the Eq. (5).

$$\hat{S}_{sim}[i, k] = \tanh \left(\sum_{m=1}^{d_{se}} (H_{Vis}[i, m] + H_{Text}[i, m]) \right) \quad (5)$$

Here, i is the index that ranges over the d dimensions of the feature vectors, and k is the index for the d_{se} dimensions of the shared space. The index m is used for the summation, which ranges from 1 to d_{se} . Each element $\hat{S}_{sim}[i, k]$ of the resulting matrix represents the tanh of the sum of the m -th elements of the i -th row of H_{Vis} and H_{Text} .

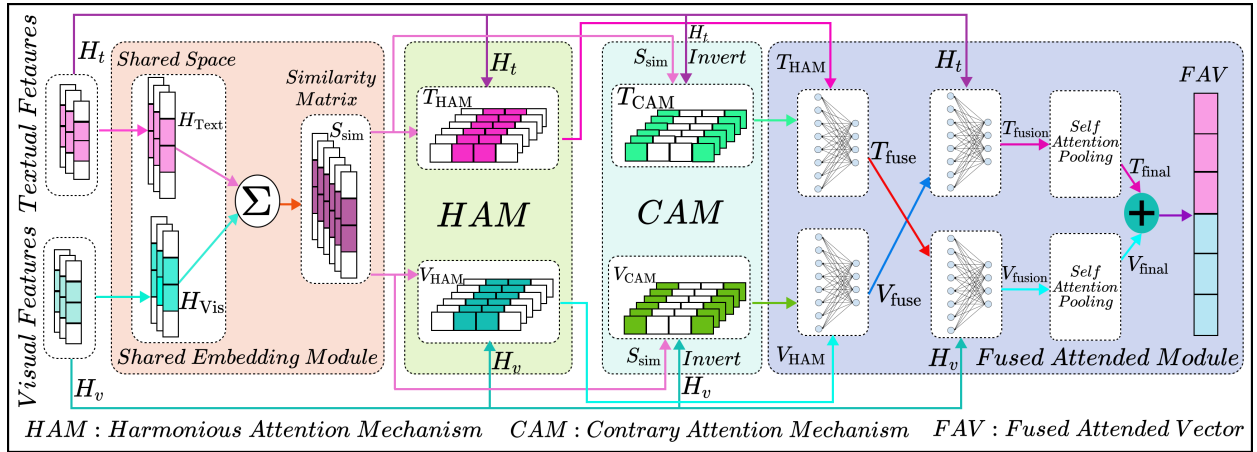


Figure 2: Inverted Dual Embedded Attention (IDEA)

Subsequently, a linear transformation is applied using the trainable weight matrix $W_{\text{sim}}[k, j] \in \mathbb{R}^{d_{\text{se}} \times d}$ to learn the importance of different elements in the similarity computation. The final similarity matrix S_{sim} can be expressed as shown in the Eq. (6).

$$S_{\text{sim}}[i, j] = \sum_{k=1}^{d_{\text{se}}} \hat{S}_{\text{sim}}[i, k] \cdot W_{\text{sim}}[k, j] \quad (6)$$

In the similarity matrix $S_{\text{sim}}[i, j] \in \mathbb{R}^{d \times d}$, every element in row i captures the degree of similarity between the i -th visual feature and the entire set of textual features. Correspondingly, each element in column j quantifies the similarity between the j -th textual feature and the entire set of visual features.

Recent research studies [40, 41] have predominantly focused on using attention matrices to evaluate co-attention weights by comparing similarities among different modalities. In contrast, our approach, ‘‘Inverted Dual Embedded Attention (IDEA)’’, does things differently. It calculates attention in a way that highlights differences and similarities, helping us understand how individual aspects of one type of information relate to the whole set of aspects of another type. It captures the hidden and complex information via two attention mechanisms, the Harmonious Attention Mechanism (HAM) and the Contrary Attention Mechanism (CAM), as shown in Fig. 2.

3.1.3.2. Harmonious Attention Mechanism (HAM): Harmonious attention mechanism emphasizes the alignment and correlation between features or information from different modalities. It is used to identify and highlight shared or similar aspects of the data. In a multimodal sentiment analysis task, harmonious attention is defined as the part that looks at words in a text description and elements in an accompanying image that express the same emotional sentiment. This aligns textual and visual cues associated with sentiment effectively. The harmonious attention vector facilitates the identification of highly correlated features between the two modalities. So, in a harmonious attention mechanism, we obtain the visual-guided textual features and vice versa. The visual-enriched textual features are obtained by applying the softmax function to the similarity matrix. This process yields attention weights, which are subsequently multiplied by the textual features. We introduce a temperature parameter T in the softmax function to control the softness or sharpness of the probability distribution[42]. A higher temperature encourages a softer, more uniform probability distribution, while a lower temperature value results in a sharper, more peaked probability distribution [43, 44]. For HAM, a higher temperature might lead to more evenly spread attention over the elements of the similarity matrix, whereas a lower temperature might result in more focused attention on a few specific elements. After rigorous experimentation, the value of T for HAM is 1.65, and for CAM, it is 0.75. We obtain the attention weights or scores

as expressed in Eq. (7):

$$(Att_{\text{weights}})_{i,j} = \frac{\exp\left(\frac{S_{\text{sim},i,j}}{T}\right)}{\sum_{k=1}^d \exp\left(\frac{S_{\text{sim},i,k}}{T}\right)} \quad (7)$$

Att_{weights} is a matrix where each element $(Att_{\text{weights}})_{i,j}$ represents the attention weight for the corresponding element in the similarity matrix S_{sim} along axis i . The visual-enriched textual features $T_{\text{HAM}} \in \mathbb{R}^{d \times dt}$ can be computed as shown in the Eq. (8)

$$T_{\text{HAM}} = \sum_{j=1}^d (Att_{\text{weights}})_{i,j} \cdot (H_t)_{j,k} \quad (8)$$

T_{HAM} is the attended representation matrix obtained after the attention mechanism. It represents the weighted combination of textual features H_t based on the attention weights $(Att_{\text{weights}})_{i,j}$.

Similarly, the textual-enriched visual features $V_{\text{HAM}} \in \mathbb{R}^{d \times dv}$ are computed by employing the softmax function on the similarity matrix to produce attention weights, which are then multiplied by the visual features. Since the attention weights $(Att_{\text{weights}})_{i,j}$ have already been computed in Eq. (7), we will use the same attention weights for the computation of V_{HAM} as shown in Eq. (9).

$$V_{\text{HAM}} = \sum_{j=1}^d (Att_{\text{weights}})_{i,j} \cdot (H_v)_{j,k} \quad (9)$$

In summary, the primary purpose of HAM is to capture and magnify the areas where information from different modalities aligns or agrees.

3.1.3.3. Contrary Attention Mechanism (CAM): Contrary attention highlights differences and disparities between features or information from different modalities. It is used to identify and accentuate areas where modalities diverge or provide contrary information. In a multimodal content moderation task, contrary attention might identify text and image content that contradict each other, helping the model detect potentially divergent content where the text and visual elements are in conflict. However, in most prior studies, contrary information, which can also be valuable for representation, is often overlooked. As shown in Fig. 2, we compute CAM using the similarity matrix and the text and image modalities after multiplying them by -1 (designated as Invert). Multiplying embeddings with -1 will reverse the direction of the embedding in the vector space. It does not alter the magnitude of the features. This can be useful for tasks such as learning to distinguish between real and fake data, generating adversarial examples, and finding various different hidden patterns. The inverted visual-enriched textual features $T_{\text{CAM}} \in \mathbb{R}^{d \times dt}$ are computed as shown in Eq. (10).

$$T_{\text{CAM}} = \sum_{j=1}^d (Att_{\text{weights}})_{i,j} \cdot (-H_t)_{j,k} \quad (10)$$

Similarly, the inverted textual-enriched visual features $V_{\text{CAM}} \in \mathbb{R}^{d \times dv}$ are computed as shown in Eq. (11):

$$V_{\text{CAM}} = \sum_{j=1}^d (Att_{\text{weights}})_{i,j} \cdot (-H_v)_{j,k} \quad (11)$$

In the context of the contrary attention mechanism, it becomes imperative to use normalization of the feature vectors because of negation. However, the harmonious attention mechanism, being a standard attention mechanism without feature negation, may not require the same normalization considerations. In summary, the primary purpose of CAM

is to capture the discrepancies, variations, or inconsistencies between modalities. It helps the model understand where and how modalities differ, contributing to a more nuanced analysis.

3.1.3.4. Fused Attended Module: To combine both harmonious and contrary attention vectors, we utilize dense layers akin to the structure found in multi-head attention [45], as illustrated below: The textually-informed visual features are computed as shown in Eq. (12):

$$V_{fuse} = \tanh((V_{HAM} \oplus V_{CAM})W_{vis} + b_{vis}) \quad (12)$$

where \oplus means concatenation operator, $V_{fuse} \in \mathbb{R}^{d \times dv}$, $W_{vis} \in \mathbb{R}^{2dv \times dv}$ and $b_{vis} \in \mathbb{R}^{1 \times dv}$ are trainable parameters.

$$T_{fuse} = \tanh((T_{HAM} \oplus T_{CAM})W_{text} + b_{text}) \quad (13)$$

where $T_{fuse} \in \mathbb{R}^{d \times dt}$, $W_{text} \in \mathbb{R}^{2dt \times dt}$ and $b_{text} \in \mathbb{R}^{1 \times dt}$ are trainable parameters. After obtaining T_{fuse} and V_{fuse} , We utilize dense layers to capture and understand the relationship that exists between the visual features and the enriched fused features. This process enables us to obtain what we refer to as the visual-fusion feature (V_{fusion}), as shown in Eq. (14).

$$V_{fusion} = \tanh((T_{fuse} \oplus H_v)\widetilde{W}_v + \widetilde{b}_v) \quad (14)$$

$V_{fusion} \in \mathbb{R}^{d \times dv}$, $\widetilde{W}_v \in \mathbb{R}^{(dt+dv) \times dv}$, and $\widetilde{b}_v \in \mathbb{R}^{1 \times dv}$ are trainable parameters.

Similarly, to obtain the textual-fusion feature (T_{fusion}), we employ dense layers to capture the correlation between the textual features and the enhanced fused features, as shown in Eq. (15).

$$T_{fusion} = \tanh((V_{fuse} \oplus H_t)\widetilde{W}_t + \widetilde{b}_t) \quad (15)$$

$T_{fusion} \in \mathbb{R}^{d \times dt}$, $\widetilde{W}_t \in \mathbb{R}^{(dt+dv) \times dt}$ and $\widetilde{b}_t \in \mathbb{R}^{1 \times dt}$ are trainable parameters.

After obtaining V_{fusion} and T_{fusion} , the next step involves extracting the most significant representation from the combined textual and visual features. We apply global average pooling to the first dimension of $T_{fusion} \in \mathbb{R}^{d \times dt}$ and $V_{fusion} \in \mathbb{R}^{d \times dv}$, the dimensions reduce to $T_{fusion} \in \mathbb{R}^{1 \times dt}$ and $V_{fusion} \in \mathbb{R}^{1 \times dv}$ respectively. It is used to reduce dimensionality, prevent overfitting, and provide a summarized representation of the feature maps. We compute the attention scores on the pooled features using a self-attention mechanism [46].

The attention score (e_i) for T_{fusion} is calculated using the scaled dot-product attention formula.

$$e_i = \frac{(T_{fusion} W_Q)(T_{fusion} W_K)^T}{\sqrt{dz}} \quad (16)$$

In Eq. (16), $W_Q \in \mathbb{R}^{dt \times dz}$ and $W_K \in \mathbb{R}^{dt \times dz}$ are parameter matrices. The term \sqrt{dz} represents the scaling factor, where dz is the dimension of the query and key spaces.

The attention weight (α_i) is obtained by applying the softmax function to the attention scores as shown in Eq. (17):

$$\alpha_i = \frac{\exp(e_i)}{\sum_{k=1}^n \exp(e_k)} \quad (17)$$

where n denotes the number of elements in the input sequence.

The final textual fused feature vector representation $T_{final} \in \mathbb{R}^{1 \times dt}$ is a weighted sum of the values based on attention weights as shown in Eq. (18):

$$T_{final} = \sum_{k=1}^n \alpha_k (T_{fusion} W_V) \quad (18)$$

where $W_V \in \mathbb{R}^{dt \times dz}$ is parameter matrix and dz is the output dimensionality, which matches that of dt .

Similarly, for V_{fusion} , repeat Eqs. (16) to (18), by replacing T_{fusion} with V_{fusion} , we can get the final representation of visual fused feature vector as $V_{\text{final}} \in \mathbb{R}^{1 \times dv}$.

After obtaining the final textual-fused feature vector T_{final} through the attention mechanism, the last step involves concatenating it with the final visual-fused feature vector V_{final} . This results in a single fused attended vector (FAV) $\in \mathbb{R}^{1 \times (dt+dv)}$ that captures the most significant representations from both textual and visual features. The concatenation operation is shown in Eq. (19).

$$FAV = T_{\text{final}} \oplus V_{\text{final}} \quad (19)$$

The fused attended vector combines the enriched information from both modalities, providing a comprehensive representation for downstream tasks such as classification. This integrated feature captures the intricate relationships between textual and visual features, enhancing the model's understanding and performance.

In summary, IDEA takes into account the similarities and dissimilarities of the textual and visual features, which in turn captures the rich representation of textual-guided visual features and visual-guided textual features. Its unique ability to discern both similar and dissimilar features enables a more comprehensive understanding of multimodal data. By dynamically allocating attention to relevant aspects in text and image inputs, IDEA excels in capturing subtle relationships, allowing the model to operate with a heightened level of context awareness. This dual capability of handling similarity and dissimilarity in patterns positions IDEA as a versatile tool in tasks such as multimodal fusion, where nuanced connections between different modalities play a crucial role. The model's adaptability to diverse patterns fosters a richer representation, enhancing its performance across a spectrum of applications. IDEA's contribution underscores the importance of attention mechanisms that go beyond the traditional focus on similarities alone. By accommodating both ends of the spectrum, IDEA serves as a testament to the evolving landscape of attention mechanisms, pushing the boundaries of what is achievable in capturing the complexities of multimodal information.

3.2. Multimodal Graph Learning

We delve into the utilization of graph-based algorithms for learning representations of both text and image data. Multimodal Graph Learning is a technique that combines graph-based representations with multiple data modalities, such as text and images. It involves constructing a graph where nodes represent different types of data and edges capture relationships. The two sub-modules of the Multimodal Graph Learning module are Multimodal Encoder and Graph Knowledge Propagation.

3.2.1. Multimodal Encoder

We discuss the feature extraction process of a multimodal encoder to create shared embedding space for both images and text. The multimodal encoder comprises two primary components: a text encoder and an image encoder. These components generate embeddings that capture the semantic relationships between images and corresponding textual descriptions. The image encoder is responsible for transforming input images into contextually enriched embeddings. On the other hand, the text encoder processes textual descriptions to produce corresponding embeddings. Utilizing transformer-based architectures, it captures contextual relationships within the text. The primary aim of the multimodal encoder is to align the embeddings of images and text within a shared semantic space. This alignment is achieved through a contrastive learning objective that encourages similar image and text pairs to have closer embeddings while pushing dissimilar pairs apart. We use a multimodal CLIP encoder [47] for this task.

3.2.2. Graph Knowledge Propagation

Graph-based knowledge propagation is the technique of disseminating information through a graph structure, where nodes signify features or data points, and edges depict relationships among them. It plays a pivotal role in tasks like information dissemination and graph-based learning. We present Algorithm 1, an approach for the construction of graphs and their knowledge propagation. The algorithm facilitates an iterative refinement of node representations of both image and text graph features. It encompasses a detailed procedure that includes the construction of graphs and the subsequent distribution of knowledge across various layers of the graph. In Algorithm 1, the operations from lines 1 to 19 are centered on constructing a similarity matrix (A). This process entails evaluating the cosine similarity between pairs of feature vectors denoted as H_i and H_j . The decision to establish an edge between feature vectors depends on whether the computed cosine similarity S_{ij} surpasses a predefined threshold (threshold ≥ 0.75). The resulting undirected edges are then incorporated into the adjacency matrix A . Consequently, lines 31 and 32 lead to the creation of two adjacency matrices: A_i , known as the Image similarity matrix, and A_t , known as the text similarity

matrix. Subsequently, from lines 20 to 30, we employ GraphSAGE (Graph Sample and Aggregated) [22] for the propagation of knowledge across the constructed matrices. It is a node embedding algorithm designed specifically to acquire representations for nodes within a graph by aggregating information from their neighboring nodes. It strikes a balance between capturing local structural information and leveraging feature information associated with nodes. The fundamental concept behind this is to generate node embeddings by gathering information from the neighboring nodes of a given node. Here, each node represents a text feature in a text similarity matrix or an image in an image similarity matrix.

Algorithm 1 Graph Construction and Knowledge Propagation

Input: Image Feature H_i (size n), Text Feature H_t (size n), $n(V_i) = n(V_t)$, K : Number of layers or depth, threshold=0.75, neighborhood function $N : V \rightarrow 2^V$.

Output: Updated node embeddings for text and image features $\forall v \in V_i$ and $\forall v \in V_t$

```

1: function SIMILARITYGRAPH( $H_i$ , threshold)
2:   Initialize adjacency matrix  $A$  with zeros
3:   for  $i = 1$  to  $n$  do
4:     for  $j = i + 1$  to  $n$  do
5:       Let  $H_i$  be the  $i$ -th feature vector
6:       Let  $H_j$  be the  $j$ -th feature vector
7:       Calculate cosine similarity between  $H_i$  and  $H_j$ :
8:        $S_{ij} = \text{cosine\_similarity}(H_i, H_j)$ 
9:       if  $S_{ij} > \text{threshold}$  then
10:        Add an edge between  $i$ -th and  $j$ -th feature vector in the adjacency matrix:
11:         $A[i][j] = 1$ 
12:        As the graph is undirected, set the symmetric entry:
13:         $A[j][i] = 1$ 
14:       else
15:        No edge between  $i$ -th and  $j$ -th feature vector below threshold:
16:         $A[i][j] = 0$ 
17:         $A[j][i] = 0$ 
18:       end if
19:     end for
20:   end for
21:   Return  $A$ 
22: end function
23: function KNOWLEDGEGRAPHPROPAGATION( $A, V, K$ )
24:   Initialize node embeddings  $h_v^0 \leftarrow (A)_v, \forall v \in V$ 
25:   for  $k = 1$  to  $K$  do
26:     for  $v \in V$  do
27:       Sample  $N(v)$  from the neighborhood of node  $v$  using the adjacency matrix  $A$ 
28:        $\text{Agg}_{N(v)}^k \leftarrow \text{Aggregate}_k(h_u^{k-1}, \forall u \in N(v))$ 
29:        $h_v^k \leftarrow \sigma \left( W_k \cdot \text{Concat}(h_v^{k-1}, \text{Agg}_{N(v)}^k) \right)$ 
30:     end for
31:     Normalize embeddings:  $h_v^k \leftarrow \frac{h_v^k}{\|h_v^k\|_2}, \forall v \in V$ 
32:   end for
33:   Return Updated node embeddings  $h_v^K$  for all  $v \in V$ 
34: end function
35:  $A_i \leftarrow \text{SIMILARITYGRAPH}(H_i, \text{threshold})$ 
36:  $A_t \leftarrow \text{SIMILARITYGRAPH}(H_t, \text{threshold})$ 
37:  $I_v \leftarrow \text{KNOWLEDGEGRAPHPROPAGATION}(A_i, V_i, K)$ 
38:  $T_t \leftarrow \text{KNOWLEDGEGRAPHPROPAGATION}(A_t, V_t, K)$ 

```

For a given node v (representing a text or an image feature) and a specific layer k , the embedding generation process in GraphSAGE consists of the following steps, as depicted in lines 21-30: Neighbor Sampling, Aggregation, and Encoding. The process commences with the initialization of node embeddings h_0^v , instantiated from the similarity matrix (A). Subsequently, the algorithm systematically advances through K layers, iteratively refining node representations. For each node v , a set of neighbors $N(v)$ is sampled from the adjacency matrix A . Information from the local neighborhood is then aggregated using a designated function $Aggregate_k$. The aggregation function can be as simple as using the mean to capture neighborhood information. This can be shown in Eq. (20).

$$Agg_{N(v)}^k \leftarrow Aggregate_k(\{h_u^{k-1}, \forall u \in N(v)\}) \quad (20)$$

where, h_u^{k-1} is the embedding of neighbor u at layer $k - 1$, and $N(v)$ is the set of sampled neighbors of node v . The updated node embeddings h_v^k are computed by concatenating the aggregation result with the prior embeddings, facilitated by a trainable weight matrix W_k . The purpose of this step is to update the embedding of the central node by considering both its local neighborhood information and its own features. This can be represented as shown in Eq. (21):

$$h_v^k \leftarrow \sigma \left(W_k \cdot \text{Concat}(h_v^{k-1}, Agg_{N(v)}^k) \right) \quad (21)$$

where, σ is an activation function (e.g., ReLU), W_k is the weight matrix for the k -th layer. This process is repeated for multiple layers k to capture different scales of neighborhood information. This process is repeated for every node till we get the updated feature of each node. The updated node embeddings are normalized after each layer to prevent gradient explosion and enforce stability and convergence. This iterative refinement process is reiterated over K layers, resulting in progressively enhanced node representations.

The ultimate output of this process manifests in the form of updated node embeddings for both image and text documents or nodes. The updated image node embeddings are denoted as I_v , as can be seen in line 33, while the corresponding updated text node embeddings are represented as T_v as can be seen in line 34. These embeddings capture nuanced representations that encapsulate information extracted from the constructed image and text similarity graphs. In summary, GraphSAGE serves as a method to aggregate embeddings from neighboring nodes for a specific target node. Each iteration results in the generation of updated node representations for every node in the graph. The application of multiple stacked layers facilitates the creation of intricate structural and semantic-level features, contributing to enhanced capabilities for various downstream tasks.

3.2.3. Graph Fusion Learning Network (GFLN)

In the Graph Fusion Learning Network, the fusion of updated text and image graph features into a unified representation is achieved through concatenation. This is done to preserve discriminative information about each modality. The choice for this concatenation approach is rooted in the fact that we aim to obtain two types of features, i.e., cross-modal features and modality-specific refined features. Cross-modal features are obtained through the IDEA mechanism, enabling the model to capture and highlight inter-modal relationships. Concurrently, the graph learning module refines modality-specific features, emphasizing unique characteristics within each modality. Due to this strategy, the model ensures the preservation of both cross-modal interactions and modality-specific nuances, contributing to a comprehensive and enriched representation of the integrated information. Following the concatenation process, the unified vector achieves a dimensionality of 1024. Subsequently, we utilize three consecutive fully connected layers: the first layer reduces the dimensionality to 512 with a dropout rate of 0.2, followed by a second layer, further reducing it to 256 with the same dropout rate. The final layer further diminishes the dimensions to 128, incorporating a dropout layer set at 0.2. This processed vector is subsequently fed into the multimodal fusion module, enabling the seamless integration of information from diverse sources.

In summary, the process begins by constructing two matrices or graphs based on cosine similarity, one for each modality. These graphs serve as input to the GraphSAGE algorithm, which updates node embeddings through iterative operations. The updated node embeddings from both modalities are fused using concatenation, preserving modality-specific features. The resulting unified vector, capturing enriched representations from both graphs, is then forwarded to the multimodal fusion module for further integration of information from distinct modalities.

3.3. Social Context Feature Extraction

In various existing works, the predominant focus has been placed solely on textual and visual features. To the best of our knowledge, none of them has extensively used Social Context Features in their model in multimodal settings to enhance crisis response. Our approach involves investigating the collective influence of textual, visual, and Social Context Features for identifying crisis-related information. Social Context Features (SCF) encompass a range of attributes, including crisis-related posts, user interaction history, etc. We have divided Social context Features into two parts: Text Semantic Profiling (TSP) and Social Interaction metrics (SIM).

3.3.1. Text Semantic Profiling

Text Semantic Profiling (TSP) is a technique that aims to decipher the contextual and conceptual facets embedded within text. TSP helps us to extract and categorize semantic attributes such as sentiment, emotions, topics, relationships, and intent. TSP includes the EmoQuotient Analysis, SentiQuotient Analysis, and Crisis Informative Score.

3.3.1.1. SentiQuotient Analysis (SentiQ): SentiQ helps in deciphering the text's subjective tone, thus contributing to a holistic interpretation of its underlying connotations. We use VADER (Valence Aware Dictionary and Sentiment Reasoner) [48] to extract the sentiments of the text. It assigns a sentiment score to each word in a piece of text. It computes a compound score that reflects the overall sentiment of the text, spanning from highly negative to highly positive, with neutrality positioned in the middle. It also provides scores for positive, negative, and neutral sentiments. By incorporating sentiment scores, models can better differentiate between classes by considering contextual sentiment and potentially weighing emotionally charged words more effectively. The SentiQ is represented as follows:

$$SentiQ = Sentiment_Encoder(T_i) \quad (22)$$

where, T_i denotes the tweets for which we must determine the sentiment expressed in the text.

3.3.1.2. EmoQuotient Analysis (EmoQ): EmoQuotient Analysis focuses on discerning emotional nuances expressed within the text, like happiness, sadness, anger, fear, etc. We use EmoLex [49] to quantitatively assess emotional content within textual data. Emotion Quotient plays a significant role in text classification by providing additional context and information about the emotional tone of the text. It gives 13 labels for a particular text. Due to this, we will get fine-grained scores for a text. These scores enhance the accuracy and granularity of the classification task. The EmoQ is represented as:

$$EmoQ = Emotion_Encoder(T_i) \quad (23)$$

where, T_i signifies the tweets for which we need to grasp the emotional tone conveyed in the text.

3.3.1.3. Crisis Informative Score (CIS): Social media text often contains spelling errors, abbreviations, user mentions, and numerous hashtags. It becomes crucial to employ a metric for categorizing informative or humanitarian content within these posts. This metric, Crisis Informative Score (CIS), assesses the semantic characteristics of text, offering a quantitative measure of crisis-related terminology within the text. To compute CIS as outlined in Algorithm 2, in line 8, we initiate the crisis lexicon count at zero. For each tweet in the dataset, we compare its content to a carefully curated lexicon containing 4,268 crisis-related terms. The number of words in a single tweet that match the crisis lexicon is tallied, as can be depicted from lines 9-15. After this process across all tweets in the dataset, we perform min-max normalization on the count of matched words within the tweets, as demonstrated in lines 16-19 of the CIS function in Algorithm 2. The CIS is represented as follows:

$$CIS = normalise(Crisis_Lexicon_Count) \quad (24)$$

where, *normalise* denotes the min-max normalization of the crisis-lexicons count present in the tweet.

3.3.2. Social Interaction Metrics (SIM)

Social Interaction Metrics are essential for understanding and analyzing how users engage with content and each other. Two significant aspects of these metrics are User Engagement Metrics (aka User Engagement Features) and User Informative Score.

3.3.2.1. *User Engagement Metrics (UEM)*: User Engagement Features encapsulate the ways in which individuals interact with content on social media. These features provide insights into the effectiveness of user content. Common user engagement features include Likes, Retweets, Replies, Followers, Friends, etc. We normalize all these scores

Algorithm 2 User-Crisis Informative Score

Input:
 U_i : Number of informative tweets posted by a user U
 U_{ni} : Number of non-informative tweets posted by a user U
 U_{Total} : Total number of tweets posted by a user U
Output:
 ϕ_c : Crisis Informative Score (CIS)

 ϕ_u : User Informative Score (UIS)

 ϕ_{u_c} : User Crisis Informative Score (UCIS)

```

1: function UIS( $U_{Total}, U_i, U_{ni}$ )
2:    $\phi_u \leftarrow \text{user\_informative\_score}(U_{Total}, U_i, U_{ni})$ 
3:    $\phi_u \leftarrow \frac{U_i - U_{ni}}{U_{Total}}$ 
4:    $\tilde{\phi}_u \leftarrow \frac{\phi_u - \min(\phi_u)}{\max(\phi_u) - \min(\phi_u)}$ 
5:   return  $\tilde{\phi}_u$ 
6: end function
7: function CIS( $\tilde{T}_i, \mathcal{L}_{lex}$ ) //  $\tilde{T}_i$  represents all the tweets present in the dataset.
8:    $count\_crisis \leftarrow 0$ 
9:   for  $t$  in  $\tilde{T}_i$  do //  $t$  is single tweet
10:    for  $w$  in  $t$  do //  $w$  represents single word in tweet
11:      if  $w$  is in  $\mathcal{L}_{lex}$  then //  $\mathcal{L}_{lex}$  is lexicon list.
12:         $count\_crisis \leftarrow count\_crisis + 1$ 
13:      end if
14:    end for
15:  end for
16:   $\phi_c \leftarrow count\_crisis$ 
17:   $\tilde{\phi}_c \leftarrow \frac{\phi_c - \min(\phi_c)}{\max(\phi_c) - \min(\phi_c)}$ 
18:  return  $\tilde{\phi}_c$ 
19: end function
20: function UCIS( $\phi_{u_c}, \tilde{\phi}_c, \tilde{\phi}_u$ )
21:    $\phi_{u_c} \leftarrow \alpha \cdot \tilde{\phi}_u + (1 - \alpha) \cdot \tilde{\phi}_c$ 
22:   return  $\phi_{u_c}$ 
23: end function

```

3.3.2.2. *User Informative Score (UIS)*: The User Informative Score is a metric designed to assess the credibility and informativeness of a user's content. It is determined by considering the following factors: the total number of tweets posted by a user denoted as U_{Total} , the number of informative tweets posted by a user denoted as U_{Info} , and the number of non-informative tweets posted by a user, represented as $U_{Non-Info}$. As depicted in Algorithm 2, lines 1-5 tell about the computation of the UIS. It can be represented as shown in Eq. (25).

$$UIS = \frac{U_{Info} - U_{Non-Info}}{U_{Total}} \quad (25)$$

The UIS metric is then normalized using min-max normalization. The Social Holistic Vector (SHV) comprises all the scores we got from Eq. (22), Eq. (23), Eq. (24), and Eq. (25).

$$SHV = \text{Concat}(\psi_e, \psi_s, \psi_u, \psi_{u^i}, \psi_{c^i}) \quad (26)$$

As shown in Eq. (26), $\psi_e, \psi_s, \psi_u, \psi_{u^i}, \psi_{c^i}$ represent the Emotion Quotient, Sentiment Quotient, User Engagement Metrics, User Informative Score, and Crisis Informative Score respectively.

3.3.2.3. User-Crisis Informative Score (UCIS): It is important to highlight that we employ a weighted sum approach, outlined in Algorithm 2, to combine the Crisis Information Score (CIS) and User Information Score (UIS). The weighted sum approach, where each score is assigned a specific weight, ensures a balanced consideration of the dual aspects, with CIS capturing the relevance of crisis content and UIS gauging the credibility of the user. This method provides flexibility by allowing adjustments to the weights, reflecting the relative importance of each aspect based on specific assessment goals or evolving contextual priorities. The resulting combined score offers a more nuanced and comprehensive measure, ultimately improving the model's ability to discern reliable and informative content during crises.

3.4. Multimodal Fusion Network (MFN)

In this section, we elaborate on the Multimodal Fusion Network. Fig. 1 illustrates different constituents of the MFN module. This module comprises four sub-modules, namely, (a) Multimodal Adaptive Learning Network, (b) Social Contextual Learning Network, (c) Joint Fusion Learning Network, and (d) Prediction Layer.

3.4.1. Multimodal Adaptive Learning Network (MALN)

In this module, the fused attended vector (FAV) further refines and distills the integrated features by learning higher-level patterns and relationships that are specific to the classification task. The network can extract informative features and establish inter-dependencies between textual and visual features, ultimately enhancing the predictive capabilities of the model. The Fused Attended Vector (FAV), initially with dimensions of 1792, undergoes a hierarchical reduction in dimensionality. It passes through successive fully connected layers, achieving dimensions of 1024, 512, 256, and 128, respectively. Each layer incorporates a dropout rate of 0.2. The refined output is then directed to the Joint Fusion Learning Network for further processing.

3.4.2. Social Holistic Learning Network (SHLN)

The Social Holistic Vector (SHV) consolidates semantic text information and social interaction information, where the latter encompasses user engagement information and user-generated informative content shared on social media platforms. The user engagement data, including favorites count, retweet count, followers count, friends count, and status count, undergoes initial scaling using min-max normalization. This processed vector is referred to as the user engagement metrics. Similarly, user-generated informative content undergoes scaling through min-max normalization, yielding the User Informative Score (UIS), as outlined in Section 3.3. The semantic textual information encompasses emotional, sentimental, and Crisis Informative Score (CIS). Following the concatenation of these processed feature vectors, the resulting comprehensive representation is denoted as the Social Holistic Vector, characterized by dimensions totaling 21. Specifically, it consists of 3 dimensions for sentiment, 11 for emotion, 1 for CIS, 5 for user engagement, and 1 for UIS. SHV encapsulates a holistic view of user interaction and content-related information on social media platforms. The SHV undergoes an initial processing stage by traversing through a fully connected layer, where its dimensions are effectively reduced to 16. To mitigate overfitting, a dropout of 0.2 is applied during this layer. Subsequently, another fully connected layer is employed, reducing the dimensions to 8 while maintaining the dropout rate at 0.2. These transformation includes dimensionality adjustments and the introduction of non-linearity through activation functions such as ReLU, enabling the network to capture intricate data patterns. During this process, the network extracts high-level features relevant to the classification task, including patterns related to user engagement, informative content, emotional and sentimental aspects. The resulting output represents a refined and condensed representation of the combined social and text information. This output is given to the Joint Fusion Learning Network.

3.4.3. Joint Fusion Learning Network (JFLN)

The feature vectors generated by MALN, SHLN, and GFLN are concatenated for joint representation. This integration enables the neural network to comprehensively capture the essence of multimodal data by merging diverse information streams. The joint representation encodes inter-modality relationships and interactions, allowing the model to discern complex patterns and correlations that may not be apparent when considering each modality in isolation. The joint representation of feature vectors passes through several fully connected layers; their dimensions undergo a step-wise reduction from 264 to 256, implementing a dropout of 0.2. This is succeeded by the application of another layer, further reducing the dimensions to 128 while maintaining a dropout rate of 0.2. The subsequent fully connected layer continues this reduction to 64 dimensions, maintaining the same dropout rate. This consolidated representation of the feature vectors is optimized for the classification task, empowering the model to make more accurate predictions by leveraging collective knowledge from all modalities, including the social context.

3.4.4. Prediction Layer

In the process of classifying content for the Informative Task, the model generates predicted class labels by passing the JFLN module's output to the prediction layer. This layer employs a Sigmoid activation function to compute predicted probabilities, mapping real-valued inputs to probabilities between 0 and 1. Model performance is assessed using binary cross-entropy loss, and the Adam optimizer updates model weights based on loss gradients. The predicted probabilities are subsequently transformed into binary labels (0 or 1) using a thresholding function. If the probability surpasses or equals the threshold ≥ 0.5 , it's assigned the label 1, denoting the Informative class; otherwise, it's labeled 0, indicating the non-informative class. This binary classification approach effectively distinguishes between informative and non-informative content.

$$L = -\frac{1}{N} \sum_{i=1}^N (y_i \log(p_i) + (1 - y_i) \log(1 - p_i)) \quad (27)$$

As shown in Eq. (27), N represents number of examples, your dataset, y_i represents true binary label (0 or 1) for the i -th example, p_i represents predicted probability that the i -th example belongs to class 1.

Similarly, for the Humanitarian Task, a multiclass classification challenge, we implement a Softmax activation function in the prediction layer to establish a probability distribution across multiple classes. The resulting probability vector assigns a probability value to each class. Model performance is evaluated using a suitable loss function for multiclass classification, such as categorical cross-entropy loss.

$$L = -\frac{1}{N} \sum_{j=1}^N \sum_{i=1}^C y_{ij} \log(p_{ij}) \quad (28)$$

As shown in Eq. (28), C represents number of classes, N represents Number of examples, y_i represents binary indicator (0 or 1) of whether class i is the correct classification for the example, p_i represents predicted probability assigned to class i by the model, y_{ij} represents binary indicator for class i in the j -th example, p_{ij} represents predicted probability for class i in the j -th example.

The Adam optimizer calculates gradients for loss-based weight updates and model training. In practice, the class with the highest probability in the predicted distribution is selected as the model's classification decision. This approach enables the model to effectively categorize data into one of the available classes.

In summary, CrisisSpot is delineated into four integral components for the identification of crisis-related information. The primary Feature Extraction and Interaction Module orchestrates the interaction between text and visual modalities, extracted from text and image encoder, respectively, utilizing an IDEA attention mechanism. This mechanism adeptly captures both harmonious and contrary patterns, forwarding the extracted features to the subsequent Multimodal Fusion Module. The second component is dedicated to Multimodal Graph Learning, where features extracted from a multimodal encoder undergo enrichment of node features via a GraphSAGE layer. The resultant fused vector is channeled into the Multimodal Fusion Module. The third module is centered on Social Context Feature Extraction, encompassing diverse attributes such as crisis-related posts and user interaction history. This module includes metrics such as User Informative Score (UIS), Crisis Informative Score (CIS), and User Engagement. UIS evaluates user

credibility, CIS quantifies crisis-related vocabulary presence, and User Engagement metrics capture pertinent text and user-centric information. The amalgamated features from this module are concatenated and fed into the Multimodal Fusion Module. The final module, Multimodal Fusion, processes the fused attended vector from the Feature Extraction Module and is passed through a dedicated Deep Neural Network, while a separate neural network handles the social holistic vector from the Social Context Feature Extraction Module. Outputs from these networks, in addition to graph-attended information, are further integrated through a Joint Fusion Learning Network, ultimately culminating in the prediction layer. This intricate architectural framework maximizes the synergistic utilization of textual, visual, and Social Context Features, augmenting the model's prowess in discerning crisis-related information. CrisisSpot has a parameter size of 209.6M, and for processing each sample, it achieves a real-time inference speed of 4.25 microseconds.

4. Experimental Evaluations

We present an overview of the datasets employed for experimental evaluations. Subsequently, we discuss unimodal and multimodal state-of-the-art methods for comparative analysis. Additionally, we discuss the standard evaluation metrics used to compare the performance of different approaches.

4.1. Datasets

We provide an overview of the CrisisMMD dataset. Subsequently, we introduce the data curation and annotation process for our newly created dataset, TSEqD (Turkey-Syria Earthquake Dataset).

4.1.1. CrisisMMD

The CrisisMMD dataset [34] is a valuable and comprehensive resource in the field of disaster management. It consists of a vast collection of multimodal social media posts that encompass texts and images from seven natural disaster events. The CrisisMMD dataset serves as a benchmark for evaluating the performance of state-of-the-art methods in disaster management. The number of samples from the CrisisMMD dataset utilized in our study is displayed in [Table 1](#).

Table 1

Data Distribution for Informative and Humanitarian Tasks in CrisisMMD dataset

Task	Train	Validation	Test
Informative	9601	1573	1534
Humanitarian	6126	998	955

4.1.2. TSEqD

Due to the dearth of multimodal datasets in the field of disaster management. We have curated a vast collection of social media posts comprising of texts and images from the Turkey-Syria Earthquake. The dataset, TSEqD (Turkey-Syria Earthquake Dataset), has two different sets of annotations: one for Informative Tasks and another for Humanitarian Tasks. We have chosen to adhere to the CrisisMMD dataset's consistent labeling format. The process of data curation, annotation, and the distribution of labels across various classes have been elaborated in subsequent sections.

4.1.2.1. Data Curation: We annotated a total of 10,352 tweets obtained during the period from February 6, 2023, to March 16, 2023. Our objective was to curate a dataset that captures diverse facets of the disaster, including details about affected individuals, losses resulting from destruction, and ongoing efforts to assist affected individuals. We utilized the Twitter API to collect these tweets, including their textual content, associated images, and metadata related to the tweets. This comprehensive dataset can serve as a valuable resource for future tasks that may leverage user-specific information or utilize tweet metadata for analysis and research purposes. The number of text and image samples per label in the TSEqD dataset is shown in [Table 2](#). The label distribution within the TSEqD dataset is illustrated in [Table 3](#).

4.1.2.2. Multitask Annotation: We first discuss the annotation process for *Task 1* and then *Task 2*.

4.1.2.2.1. Annotation Process for Task 1 (Informative Task): This task typically involves annotating posts to determine whether they contain valuable information, news updates, or relevant details regarding the ongoing crisis event. Informative Task annotations are essential for distinguishing between posts that contribute to situational

Table 2
Number of Text and Image Samples per Label in TSEqD Dataset

Description	Label	Text	Image
Informative	1	7136	5363
Non-Informative	0	3199	4972

Table 3
Distribution of Labels in TSEqD Dataset

Label	Count
Both Informative	4312
At least one Informative	8187
Non-Informative	2148

awareness and those that do not, aiding in the effective management of disaster response efforts. Examples of such posts are the appeals of organizations asking for support to help the victims, aid camp information, information about a lost or found individual, and reports of death tolls. The post which does not contain any disaster-related information is annotated as non-informative.

4.1.2.2.2. Annotation Process for Task 2 (Humanitarian Task): In this task, we assign labels to each tweet based on its corresponding category. We elaborate on the different categories as follows:

Infrastructure and Utility Damage: This category shows the damage to built structures, e.g., Damaged roads, destroyed buildings, rubble, and many more.

Vehicle Damage: This category shows damaged vehicles such as broken windows and cars under debris.

Rescue or Donations Efforts: This category shows donations or volunteering efforts, e.g., Transport people to safe places, evacuate, and provide medical aid.

Injured or Dead People: This category shows the information related to injured or dead people. These involve current death tolls, injuries, and deaths seen in an area describing their cause.

Affected Individuals: This category shows things such as people sitting outside, waiting in line to receive aid, needing shelter, etc.

Missing or Found People: This category shows instances of missing or found people.

Other Relevant Information: This category shows some relevant information not covered by the categories mentioned above. These may include maps of the affected areas and possible attempts of fraud or criminal activities taking place using the disaster as a cover. Also, any images that have contact information or QR codes for donations can also be included.

The distribution of text and image samples in each class in TSEqD dataset is shown in [Table 4](#). In brief, we have annotated the dataset for various tasks, such as the Informative Task (Task 1) and Humanitarian Task (Task 2). The annotated dataset, namely TSEqD, contains about 10,352 data samples. The dataset contains 22 columns and contains necessary meta information which can be helpful to the researchers. To the best of our knowledge, no such dataset in disaster management has this unique and meaningful data.

In summary, we have performed annotations for two distinct tasks: the Informative Task and the Humanitarian Task. The TSEqD dataset comprises approximately 10,352 data samples and possesses 22 columns, including essential metadata, which can be of great assistance to researchers. This dataset represents a valuable resource in the field of disaster management, offering unique and meaningful data.

4.1.2.3. Inter-Annotator Agreement: In the annotation process, we conducted separate annotations for both image and text data. The inter-annotator agreement scores for different modalities under different tasks can be seen in [Fig. 3](#). Task 1, being a binary task, displays a notably higher inter-annotator agreement, indicating minimal ambiguity in the annotation process. In contrast, Task 2 exhibits a substantial decrease in agreement, primarily due to two significant factors. First, Task 2 is dependent on Task 1, and second, the inherent complexity of Task 2 leads to various possible interpretations. Notably, Task 2 may involve cases where a single image corresponds to multiple labels, potentially

Table 4
Distribution of Text and Image Samples in Each Class in TSEqD Dataset

Description	Label	Text	Image
Infrastructure and Utility damage	1	131	1279
Vehicle Damage	2	0	46
Rescue and donation	3	4235	1659
Injured or dead people	4	1182	199
Affected Individuals	5	492	1125
Missing or found people	6	83	12
Other relevant info	7	1015	1041
Not relevant or can't judge	8	3197	4974

■ Informative Text
■ Informative Image
■ Humanitarian Text
■ Humanitarian Image

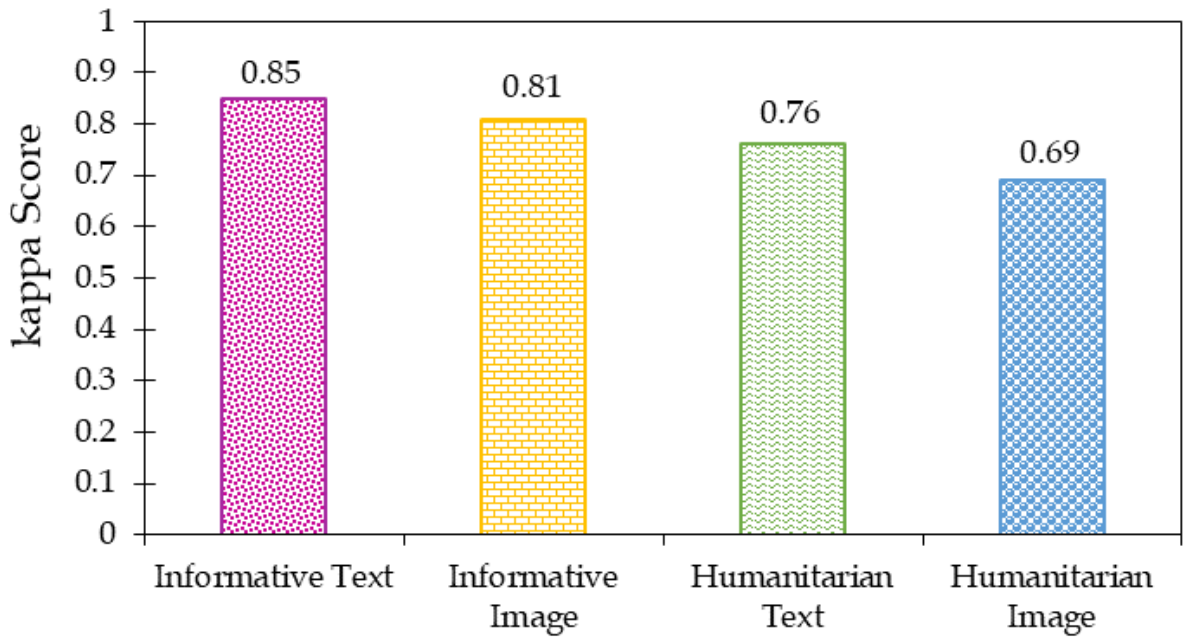


Figure 3: Inter-Annotator Scores for Informative and Humanitarian Tasks

causing discrepancies between annotators. While both tasks exhibit a moderate level of agreement, Task 2, which focuses on humanitarian images, shows significantly lower agreement compared to humanitarian text. The level of agreement and the reliable data percentage after the annotation process are shown in the [Table 5](#). The inter-annotator agreement is quantified using Cohen's Kappa coefficient, a statistical measure that accounts for chance agreement, and it is computed as follows.

$$\kappa = \frac{P_o - P_e}{1 - P_e} \quad (29)$$

As shown in [Eq. \(29\)](#), P_o is the actual agreement of the annotators. It is calculated by comparing the number of times annotators had the same annotations for given data.

P_e is the probability of the two annotators agreeing on annotation calculated by multiplying the probability of each annotator predicting a class adds for all the classes. This is deducted from the total calculation to ensure that the agreement is not by chance.

Table 5

Level of Agreement and Reliability Percentage for Calculating Kappa Scores

Kappa Value	Level of Agreement	Reliable Data(%)
0–0.20	None	0–4%
0.21–0.39	Minimal	4–15%
0.40–0.59	Weak	15–35%
0.60–0.79	Moderate	35–63%
0.80–0.90	Strong	64–81%
Above 0.90	Almost Perfect	82–100%

4.2. Creation of Crisis Lexicons

In the domain of crisis management, a well-constructed crisis lexicon list is essential, facilitating the clear and accurate communication of vital information. By integrating crisis-specific keywords in social media posts, stakeholders can efficiently sift through extensive online content, accessing pertinent information directly linked to the ongoing crisis. Olteanu *et al.* [50] formulated a lexicon list tailored to floods, encompassing 360 crisis-related terms. Additionally, we sourced 400 crisis lexicons from various online sources, such as Wikipedia⁴, and Disaster Words Vocabulary-List⁵. Our innovative approach involved leveraging a text encoder to generate embeddings for these meticulously curated crisis lexicons, along with word-level embeddings for tweets. By computing the cosine similarity between the crisis lexicon embeddings and tweet embeddings, we pinpointed words surpassing a threshold of 0.8, subsequently integrating them into the crisis lexicon list. These comprehensive crisis lexicon lists offer domain-specific insights, potentially enhancing the ability to discern pertinent content shared on social media platforms.

4.3. Comparison Methods

We explore a range of state-of-the-art unimodal and multimodal techniques. Among the unimodal methods, we delve into BERT and ResNet. For multimodal approaches, we examine state-of-the-art methods such as ViLBERT, ViLT, and VisualBERT, along with SCBD, MAN, CAMM, RoBERTaMFT, FixMatchLS_{img+eda}, and DMCC.

BERT: BERT (Bidirectional Encoder Representations from Transformers) [37] model is pre-trained on vast corpora, enabling it to capture contextual nuances and semantics, making it exceptionally effective for vast NLP tasks, including question-answering, text classification, and language understanding.

ResNet: ResNet (Residual Network) [51] model addresses the issues of vanishing gradient in deep convolutional neural networks by introducing residual connections. ResNet has established itself as a cornerstone in the field of computer vision by achieving state-of-the-art performance in image recognition tasks.

VisualBERT: VisualBERT [52] is a groundbreaking model that combines vision and language understanding by integrating the Transformer architecture with both convolutional and recurrent neural networks. It leverages pre-trained BERT embeddings alongside visual features, enabling multimodal tasks such as visual question answering and image captioning.

ViLBERT: Vision and Language BERT (ViLBERT) [53] model is a pioneering architecture that integrates visual and textual information within a single BERT-based framework. Through pre-training on vast amounts of multimodal data, ViLBERT captures nuanced relationships between vision and language, enabling it to excel in tasks like visual question answering, image-text retrieval, and image captioning.

ViLT: The ViLT (Vision-and-Language Transformer) [54] model harnesses the power of transformer architecture to seamlessly fuse textual and visual information. By jointly pre-trained on different vision and language data, ViLT achieves remarkable capabilities in tasks like image captioning, visual question answering, and cross-modal retrieval,

⁴<https://en.wikipedia.org/wiki/Earthquake>

⁵<https://www.vocabulary.com/lists/32961>

offering a versatile and powerful solution for bridging the gap between vision and language domains.

SCBD: SCBD (SSE-Cross-BERT-DenseNet) [18] model presents an approach to real-time event detection, particularly in emergency response scenarios. The model introduces a cross-attention module to filter out irrelevant components from text and image inputs, addressing the limitations of unimodal approaches. Additionally, SCBD employs a multimodal graph-based approach, allowing stochastic transitions between embeddings of different multimodal pairs during training to improve regularization and handle limited training data effectively.

MANN: Multimodal Adversarial Neural Network (MANN) [19] addresses a significant challenge in disaster-related message detection on social media by introducing an approach to identifying posts related to emerging disaster events. It has the ability to extract comprehensive features from both text and images, enabling accurate detection of disaster-related content and adaptability to unforeseen events through adversarial training.

CAMM: The Cross-Attention Multi-Modal (CAMM) [55] deep neural network is proposed for classifying multimodal disaster data on social media. Integrating text and image information from Twitter posts using attention mechanisms, CAMM employs the attention mask from the textual modality to highlight relevant features in the visual modality. This cross-attention-based method emphasizes its efficacy in capturing pertinent cross-domain features in both text and image data.

FixMatchLS_{img+eda}: FixMatchLS_img+eda [56] leverages the advantages of text and image modalities by integrating back translation and easy data augmentation techniques into the FixMatchLS model, an algorithm recognized for its semi-supervised learning capabilities. FixMatchLS_{img+eda} builds upon the foundation of the MMBT (Multimodal Bitransformers) model. To fine-tune the FixMatchLS_{img+eda} model, a dynamic weighting mechanism is introduced for the labeled and unlabeled loss components.

RoBERTaMFT: RoBERTa-based multimodal fusion transformer [57], addresses the challenges of multimodal learning. Its co-learning methodology effectively addresses issues related to recognition performance limitations and data imbalances among modalities. RoBERTaMFT is poised to offer significant advancements in multimodal understanding and classification by promoting balanced and effective learning across different data modalities.

DMCC: Deep Multimodal Crisis Categorization Framework (DMCC) [58] employs a two-level fusion strategy to seamlessly integrate textual and visual data. At the feature level, the MCA block ensures an effective fusion of these modalities. This holds the potential to enhance real-time crisis assessment and resource allocation, offering valuable support to emergency responders in dynamic and evolving situations.

4.4. Evaluation Metrics

In our study, we assess a model's effectiveness using well-defined metrics such as accuracy, precision, recall, and F1-score. Accuracy offers a general measure of correctness. Precision evaluates the accuracy of positive predictions, while recall gauges the model's ability to correctly identify positive instances. The F1-Score, a harmonic mean of precision and recall, provides a balanced evaluation by considering both false positives and false negatives.

4.5. Experimental Results

We first present the experimental setup, then present our experimental results and perform comparative assessments across various datasets. Initially, we compare the results of our proposed method with unimodal methods such as BERT [37], and ResNet [51]. Subsequently, we compare our proposed method with multimodal state-of-the-art methods, such as VisualBERT [52], ViIT [54], ViLBERT [53]. SCBD[18], MANN[19], CAMM[55], FixMatchLS_{img+eda} [56], RoBERTaMFT [57], and DMCC [58]. Furthermore, we conduct a comprehensive evaluation to determine the performance improvements associated with each modality and constituent component integrated into our proposed model.

4.5.1. Experimental Setup

In this study, all neural models are implemented using the PyTorch and TensorFlow frameworks, executed on a Linux server equipped with an Intel(R) Xeon(R) Silver 4215R CPU @3.20 GHz, 256GB of RAM, and a 16GB NVIDIA

Tesla T4 GPU. The pre-trained BERT, CLIP, and ResNet models are accessible through the Hugging Face repository. We adopt the Adam optimizer and set the learning rate hyper-parameter for the model to $5e - 5$. For the Feature Extraction and Interaction module (FEIM), we configure the dimensionality of hidden representations to $d = 768$ for the textual modality and 1024 for the visual modality. Similarly, for the Multimodal Graph Learning module (MGLM), the dimensionality of hidden representations for both textual and visual modalities is set to $d = 512$. To mitigate overfitting, a dropout rate of 0.2 is applied. The training process is conducted over 100 epochs.

4.5.2. Network Hyperparameters

In this section, we systematically explore hyperparameters for our proposed model, such as learning rate, epochs, dropout, batch size, and optimizer, with the goal of identifying optimal configurations for improved training and overall performance. For the learning rate, we conducted comprehensive experiments across a range from $5e - 1$ to $5e - 7$ to identify the most effective rate for optimal model performance. Subsequently, after thorough evaluation, we determined that a learning rate of $5e - 5$ yielded the best results, and this value was consequently adopted as part of our finalized configuration. The exploration of epochs involved intentional variations, considering values of 50, 80, 100, and 120. Through systematic experimentation, we observed that setting the number of epochs to 100 provided the optimal balance between model convergence and performance enhancement. As a result, 100 epochs were selected and incorporated into our final hyperparameter configuration. In addressing the batch size, we systematically evaluated sizes of 16, 32, 64, and 128 to accommodate diverse computational resources and memory constraints. After a thorough assessment, a batch size of 32 emerged as the choice that delivered the best results, aligning with our commitment to optimizing model performance under varied conditions. The exploration of dropout rates involved testing values within the range of 0.2 to 0.5. After careful consideration of performance metrics, a dropout rate of 0.2 was identified as optimal, providing an effective regularization mechanism without compromising the model's learning capacity. Throughout the experimentation process, the optimizer emerged as a critical component influencing model performance. After evaluating various options, Adam stood out as the preferred optimizer, demonstrating significant performance in optimizing the learning process of our model.

In summary, our finalized hyperparameter configuration includes a learning rate of $5e - 5$, a selected batch size of 32, 100 epochs, a dropout rate of 0.2, and the utilization of the Adam optimizer during the model training process. These choices represent the culmination of rigorous experimentation aimed at achieving the optimal balance in model performance.

4.5.3. Performance Comparison on CrisisMMD

To determine how well our proposed model performs, we conducted a comprehensive evaluation by comparing CrisisSpot to both unimodal and multimodal state-of-the-art methods. We used the CrisisMMD dataset [34] for this assessment. We measured the performance of these methods using well-established metrics as discussed in Section 4.5.3. The results present in Table 6 and Table 7 clearly show that CrisisSpot significantly outperforms both the unimodal and multimodal state-of-the-art methods. These findings provide strong evidence to support the effectiveness of our proposed approach.

4.5.3.1. Performance Comparison for Informative Task

To affirm the effectiveness of CrisisSpot in addressing the Informative Task on the CrisisMMD dataset [34], we carried out a thorough comparative analysis against unimodal and multimodal state-of-the-art approaches, as outlined in Table 6. Our proposed approach yielded impressive results, with an accuracy of 97.58% and an F1-score of 98.23% for the Informative Task. Notably, our approach surpassed both the unimodal and multimodal state-of-the-art benchmarks by a significant margin.

Transformer-based models, such as VisualBERT [52], ViLT [54], and ViLBERT [53], are renowned for their capabilities in addressing multimodal classification problems by efficiently handling text-image pairs and providing enhanced contextual embeddings. In our proposed approach, we harness the power of these transformer-based techniques, coupled with the incorporation of text-semantic scores and user engagement metrics within our model. Notably, our method surpasses VisualBERT by 9.48%, 10.41%, 12.57%, and 11.47% across all evaluation metrics. Similarly, our method, CrisisSpot, outperformed ViLBERT, achieving an accuracy improvement of 9.33%, precision enhancement of 7.78%, recall improvement of 9.66%, and an F1-score increase of 8.70%. Furthermore, in comparison to ViLT, our approach excelled with an accuracy improvement of 9.98%, precision improvement of 8.41%, recall enhancement of 10.62%, and an F1-score increase of 8.50%.

Table 6
Performance Comparison on CrisisMMD for Informative Task

Model	Acc	Prec	Rec	F1
BERT [37]	86.22	86.01	86.22	86.11
ResNet [51]	84.88	84.76	84.89	84.82
Visual BERT [52]	88.10	86.29	87.23	86.76
ViLT [54]	87.60	88.29	89.18	88.73
ViLBERT [53]	88.25	88.92	90.14	89.53
SCBD [18]	88.52	91.13	91.84	91.48
MANN [19]	84.09	86.38	90.58	88.43
CAMM [55]	87.22	89.56	91.65	90.59
FixMatchLS _{img+eda} [56]	-	91.00	90.80	90.50
RoBERTaMFT [57]	88.90	-	-	87.40
DMCC [58]	92.24	92.24	92.23	92.23
CrisisSpot	97.58	96.70	99.80	98.23

Furthermore, when CrisisSpot is compared to other state-of-the-art methods, it demonstrated significant performance, clearly highlighting its substantial improvements in all the evaluation metrics as mentioned in Section 4.4. We also conducted comparisons with FixMatchLS_{img+eda} [56], RoBERTaMFT [57], and DMCC [58]. In these evaluations, our method notably exhibited a substantial performance enhancement, registering substantial improvements of 5.70% in precision, 9.0% in recall, and 7.73% in F1-score when compared to FixMatchLS_{img+eda}. In the case of RoBERTaMFT, a method that employs co-learning between text and image to address recognition limitations and data imbalance, our approach outperformed it by 8.68% in accuracy and 10.83% in the F1-score. When compared to DMCC, we witnessed an improvement of 5.34% in accuracy, 4.46% in precision, 7.57% in recall, and 5.99% in F1-score. Additionally, we compare CrisisSpot with SCBD[18], MANN[19], and CAMM[55] in which our method surpasses all these multimodal state-of-the-art methods by significant margins across all the evaluation metrics. We attribute this performance enhancement to the incorporation of graph-based learning, which enriches the feature representation of modalities. Furthermore, our proposed attention mechanism, IDEA, enabled the model to capture both similar and dissimilar pairs more effectively, facilitating its ability to attend to essential patterns. Our model captures both modality-specific features and cross-modal relationships, contributing to the improved performance of our model. Additionally, the integration of Social Contextual Features enhanced the model's context understanding by augmenting it with text-centric and user-centric scores. These comprehensive comparisons underscore the robust performance of CrisisSpot in the domain of disaster management. We have used various notations for evaluation metrics: accuracy as (Acc), precision as (Prec), recall as (Rec), and F1-Score as (F1). All these metrics are presented in percentage (%) in all the Tables of the paper.

4.5.3.2. Performance Comparison for Humanitarian Task

We performed a performance comparison of CrisisSpot with unimodal and multimodal state-of-the-art models for humanitarian tasks using the CrisisMMD dataset [34] as shown in Table 7. While there are various state-of-the-art models for classifying disaster-related tweets, many of them do not utilize the official data split provided by the CrisisNLP repository [59, 60]. Consequently, we focus our comparison on those methods that adhere to the official data split. Notably, CrisisSpot surpasses VisualBERT [52] by substantial margins, achieving improvements of 5.96% in accuracy, 8.65% in precision, 6.48% in recall, and 7.25% in F1-score. Similarly, we outperform ViLBERT [53], showcasing an accuracy gain of 5.68%, a precision enhancement of 5.92%, a recall improvement of 3.52%, and an F1-score increase of 4.40%. Additionally, compared to ViLT [54], our approach excels with a 6.71% accuracy improvement, 7.05% precision enhancement, 5.12% recall enhancement, and a 5.76% F1-score increase. Additionally, our method exhibited a performance improvement of 2.87% in precision, 2.14% in recall, and 2.33% in F1-score when compared to FixMatchLS_{img+eda} [56]. In comparison to RoBERTaMFT, [57], our method demonstrated a significant performance improvement, with a 5.11% increase in accuracy and a 9.73% enhancement in the F1-score. Finally, our proposed approach outperformed DMCC [58], demonstrating a performance gain of 2.01% in accuracy, 2.75% in precision, 2.24% in recall, and 2.14% in F1-score. Furthermore, we benchmark CrisisSpot against SCBD[18],

MANN[19], and CAMM[55], demonstrating that our approach outperforms these multimodal methods by substantial margins across all evaluation metrics. It is important to highlight that the humanitarian task entails multi-class

Table 7
Performance Comparison on CrisisMMD for Humanitarian Task

Model	Acc	Prec	Rec	F1
BERT [37]	81.25	82.13	82.72	82.42
ResNet [51]	81.33	81.29	81.98	81.63
Visual BERT [52]	84.05	82.22	83.56	82.88
ViT [54]	83.30	83.82	84.92	84.37
ViLBERT [53]	84.33	84.95	86.52	85.73
SCBD [18]	80.62	80.77	80.52	80.64
MANN [19]	78.42	78.59	78.42	78.50
CAMM [55]	82.19	82.31	81.88	82.09
FixMatchLS _{img+eda} [56]	-	88.00	87.90	87.80
RoBERTaMFT [57]	84.90	-	-	80.40
DMCC [58]	88.00	87.95	87.80	87.72
CrisisSpot	90.01	90.87	90.04	90.13

classification, posing a challenge due to uneven label distributions. Notably, our proposed approach achieves notable performance improvements over existing models, even without employing data augmentation to balance the dataset. This improvement can be attributed to our incorporation of word-level and sentence-level features. This approach considers both local and global contexts within the modalities, resulting in a richer context that ultimately enhances the overall model performance. Additionally, the incorporation of semantic text features such as emotion features, sentiment features, the Crisis Informative Score, and various social interaction scores further enhances the model's understanding of the context. In conclusion, these thorough comparisons highlight the effectiveness of CrisisSpot within the realm of disaster management.

4.5.4. Performance Comparison of TSEqD

To validate the effectiveness of CrisisSpot, we have compared it with existing unimodal and multimodal state-of-the-art benchmarks on our TSEqD dataset.

4.5.4.1. Performance Comparison for Informative Task

We have conducted a comparative analysis of CrisisSpot against both unimodal and multimodal state-of-the-art models. As indicated in Table 8, CrisisSpot achieved an accuracy of 84.42%, a precision of 84.57%, a recall of 96.20%, and an F1-score of 90.01% for the Informative Task. CrisisSpot exhibited substantial performance in comparison to unimodal and multimodal state-of-the-art benchmarks, demonstrating significant improvements in all evaluation metrics as discussed in Section 4.4. Moreover, our results are compared with those of FixMatchLS_{img+eda} (referenced in [56]), RoBERTaMFT (cited in [57]), and DMCC (mentioned in [58]). Furthermore, CrisisSpot displayed noteworthy improvements, surpassing FixMatchLS by 5.70% in precision, 9.0% in recall, and 7.73% in F1-score. In the case of RoBERTaMFT, our approach outperformed it by 8.68% in accuracy and 10.83% in the F1-score. Additionally, when compared to DMCC, our method exhibited performance gains of 3.32% in accuracy and 0.42% in precision, 6.07% in recall, and 2.98% in F1-score. Furthermore, we benchmark CrisisSpot against SCBD[18], MANN[19], and CAMM[55], demonstrating that our approach outperforms all these multimodal state-of-the-art methods by substantial margins across all evaluation metrics. These comprehensive comparisons underscore the effectiveness of our CrisisSpot in the context of disaster content classification.

4.5.4.2. Performance Comparison for Humanitarian Task

We have performed a comparative analysis of CrisisSpot, evaluating it against both unimodal and multimodal state-of-the-art methods in the context of Humanitarian Tasks. As depicted in Table 9, our method achieves an accuracy of 80.55%, a precision of 81.87%, a recall of 82.20%, and an F1-score of 82.03% for the Humanitarian Task. Our method outperforms both the unimodal and multimodal state-of-the-art benchmarks by significant margins.

Table 8
Performance Comparison on TSEqD for Informative Task

Model	Acc	Prec	Rec	F1
BERT [37]	76.42	78.29	79.35	78.81
ResNet [51]	77.85	79.54	80.23	79.89
Visual BERT [52]	78.56	80.21	81.28	80.74
ViIT [54]	78.92	79.65	81.28	80.45
ViLBERT [53]	79.99	82.24	86.86	84.48
SCBD [18]	80.79	83.16	89.58	86.25
MANN [19]	80.14	82.76	88.55	85.55
CAMM [55]	81.08	83.89	90.34	86.99
FixMatchLS _{img+eda} [56]	80.23	82.95	89.96	86.31
RoBERTaMFT [57]	78.23	82.55	88.25	85.30
DMCC [58]	81.10	84.15	90.13	87.03
CrisisSpot	84.42	84.57	96.20	90.01

Table 9
Performance Comparison on TSEqD for Humanitarian Task

Model	Acc	Prec	Rec	F1
BERT [37]	72.22	74.44	75.84	75.13
ResNet [51]	72.85	75.54	76.23	75.88
Visual BERT [52]	74.56	76.21	78.28	77.23
ViIT [54]	74.02	75.23	78.25	76.71
ViLBERT [53]	76.00	78.27	80.19	79.22
SCBD [18]	77.50	78.03	78.58	78.30
MANN [19]	76.80	77.25	78.95	78.09
CAMM [55]	78.00	79.43	80.34	79.88
FixMatchLS _{img+eda} [56]	75.23	74.95	78.96	77.01
RoBERTaMFT [57]	71.23	74.55	78.25	76.36
DMCC [58]	78.10	77.15	78.80	77.96
CrisisSpot	80.55	81.87	82.20	82.03

Furthermore, we assessed our results in comparison to FixMatchLS (referenced in [56]), RoBERTaMFT (cited in [57]), and DMCC (mentioned in [58]). Our method exhibited performance improvements over FixMatchLS by 8.32% in accuracy, 6.92% in precision, 3.24% in recall, and 4.07% in F1-score. When compared to RoBERTaMFT, CrisisSpot shows significant improvements of 9.32% in accuracy, 7.32% in precision, 3.4% in recall, and 5.67% in F1-score, respectively. Furthermore, in comparison to DMCC, our method demonstrated performance gains of 2.45% in accuracy, 4.72% in precision, 3.4% in recall, and 4.07% in F1-score. Furthermore, we benchmark CrisisSpot against SCBD[18], MANN[19], and CAMM[55], demonstrating our method’s substantial performance improvements across all evaluated metrics compared to these multimodal approaches. These comprehensive comparisons underscore the strong performance of CrisisSpot.

4.5.5. Performance Gain Analysis

We assess the performance improvement achieved by CrisisSpot through a systematic analysis. Initially, we evaluate our model’s performance with different combinations of modalities and subsequently explore the impact of the attention mechanism. Subsequently, we evaluated the effect of incorporating different combinations of Social Context Features in our method.

4.5.5.1. Analyzing Combinations of Modalities

We scrutinize the performance of the CrisisSpot using diverse combinations of modalities. Due to the varying nature

of the different modalities, it becomes imperative to analyze the effect of various combinations of modalities used in our approach. The inputs to our method encompass three distinct modalities: textual modality (T), visual modality (I), and Social Context Features (SCF). The performance comparisons of these diverse modality combinations are detailed in Table 10.

Table 10
Modality-based Comparison on Informative Task

Model	Acc	Pre	Rec	F1
CrisisSpot (w/o Image)	91.72	92.20	94.66	93.41
CrisisSpot (w/o Text)	92.56	93.84	95.35	94.14
CrisisSpot (w/o SCF)	94.63	95.86	96.42	96.14
CrisisSpot (T+I+SCF)	97.58	96.70	99.80	98.23

'T' and 'I' represent Text and Image respectively.

CrisisSpot (I+T+SCF) represents our proposed method as shown in Table 10, encompassing all three modalities. To assess the significance of the image input, we exclude it while preserving text and Social Context Features, resulting in the model CrisisSpot (w/o Images). Similarly, the CrisisSpot (w/o Text) model utilizes images and Social Context Features as input, omitting text data. Furthermore, to highlight the importance of Social Context Features, we exclude them from our model. This version is referred to as CrisisSpot (w/o SCF), using text and images as inputs.

The CrisisSpot (w/o SCF) exhibits substantial performance compared to the CrisisSpot (w/o image) with improvements of 2.9% in accuracy, 3.66% in precision, 5.14% in recall, and 5.09% in F1-score, respectively. This improvement can be attributed to the comprehensive consideration of both modalities in the CrisisSpot (w/o SCF). In the CrisisSpot (w/o image), the focus is primarily on textual and Social Context Features, which limits its performance. Additionally, an attention mechanism was not applied in the CrisisSpot (w/o image) due to the presence of only a single modality.

CrisisSpot (T+I+SCF), which combines textual modality, visual modality, and Social Context Features, outperforms all other variants across all evaluation metrics. In comparison, CrisisSpot (T+I+SCF) exhibits a significant performance boost, surpassing CrisisSpot (w/o SCF) by 2.73% in accuracy, 0.84% in precision, 3.38% in recall, and 2.09% in F1-score. Moreover, it outperforms CrisisSpot (w/o Text) by 2.95% in accuracy, 2.84% in precision, 4.45% in recall, and 4.09% in F1-score. This significant enhancement in the CrisisSpot (T+I+SCF) compared to its variants comes from the effective utilization of multimodal information and Social Context Features present in the posts. These results underscore the efficiency of our proposed multimodal approach and emphasize the significance of each modality employed in the model.

4.5.5.2. Analysis of Inference Time

Inference is the stage where a trained model makes predictions or classifications based on input data. Inference time refers to the time taken by the model to make the predictions. We measure inference time in milliseconds (ms). In Table 11, we present an analysis of inference time demonstrated by various models. Two distinct temporal metrics are under consideration: Total Inference Time (TIT), indicating the overall time needed for processing all batches, and Per Sample Inference Time (PSIT), representing the duration for processing individual samples. The proposed CrisisSpot model exhibits a low inference time compared to SCBD, FixMatchLS_{img+eda}, RobertaMFT, ViLBERT, and VisualBERT. However, it shows a relatively high inference time compared to other state-of-the-art methods. This can be attributed to CrisisSpot's distinctive feature of integrating three neural networks, leading to an increase in inference time. Additionally, the inclusion of the Inverted Dual Embedded Attention (IDEA) mechanism, designed to capture both harmonious and contrary information patterns, contributes to a slight computational overhead. Although the inference time of our model is slightly higher than some of the state-of-the-art methods, it achieves the highest performance in terms of all evaluation measures.

4.5.5.3. Analysis of Attention Mechanism

We conducted a performance analysis of CrisisSpot with and without an attention mechanism. We denote our proposed model with attention as CrisisSpot (With Att) and without attention as CrisisSpot (W/o Att).

CrisisSpot (w/o Att): It refers to the implementation of the proposed model without attention applied to both textual modality and visual modality. Here, we did not apply any kind of attention to the text and image features, resulting in

Table 11
Analysis of Inference Time

Model	TIT(ms)	PSIT(ms)
BERT [37]	2685	1.75
ResNet [51]	1427	0.93
CAMM [55]	2823	1.84
ViIT [54]	3636	2.37
MANN [19]	4495	2.93
DMCC [58]	4541	2.96
SCBD [18]	6903	4.50
FixMatchLS _{img+eda} [56]	7854	5.12
RoBERTaMFT [57]	7517	4.90
ViLBERT [53]	8437	5.50
Visual BERT [52]	9971	6.50
CrisisSpot	6520	4.25

TIT: Total Inference Time, PSIT: Per Sample Inference Time
Number of samples: 1534

not capturing the complex interactions between textual and visual modalities. The resulting model gets an accuracy of 95.86%, precision of 94.32%, recall of 98.72, and F1-score of 96.47% as shown in Table 12.

Table 12
Attention-based Comparison for Informative Task

Model	Acc	Prec	Rec	F1
CrisisSpot (w/o Att)	95.86	94.32	98.72	96.47
CrisisSpot (with Att)	97.58	96.70	99.80	98.23

CrisisSpot (with Att): This description relates to the implementation of our proposed approach with an attention mechanism applied to multimodal content. In this particular variant, attention is applied to the word embeddings obtained from the text encoder based on transformers and the image embeddings from the image encoder. This attention mechanism is utilized to identify both similar and dissimilar patterns within the data. As the CrisisSpot (with Att) models the interaction between the text and image modalities, it achieves an accuracy of 97.58%, precision of 96.70%, recall of 99.80, and F1-score of 98.23%, as shown in Table 12.

4.5.5.4. Analysis of Social Context Features

We demonstrate the significance of the Social Context Features (SCF) employed in the CrisisSpot. The SCF discussed in this section are User Informative Score (UIS), Crisis Informative Score (CIS), and other features. We denote the proposed model without User Informative Score as CrisisSpot (w/o UIS). Similarly, we denote the proposed model without Crisis Informative Score as CrisisSpot (w/o CIS), and the proposed model without other features as CrisisSpot (w/o other features). The other features refer to the Sentiment Quotient, Emotion Quotient, and User Engagement Metrics.

CrisisSpot (w/o UIS): As shown in Table 13, the CrisisSpot (w/o UIS) attains an accuracy of 96.08%, a precision of 95.23%, a recall of 98.31%, and an F1-score of 96.74%. The omission of User Informative Score (UIS) integration in our model has resulted in the neglect of user credibility assessment. Extensive experimentation has demonstrated the pivotal role UIS plays in assessing the informativeness of social media content during disaster events. A high UIS score indicates that a user is contributing more substantiated and informative content.

CrisisSpot (w/o CIS): As demonstrated in Table 13, the CrisisSpot (w/o CIS) attains an accuracy of 97.03%, a precision of 96.18%, a recall of 99.21%, and an F1-score of 97.67%. The absence of the Crisis Informative Score in our approach implies that we are overlooking the significance of crisis-related vocabulary within a text. The CIS score essentially measures the presence of crisis-related words in a given text. A higher CIS score indicates that the text contains a

Table 13
Social Context Feature-based Comparison for Informative Task

Model	Acc	Prec	Rec	F1
CrisisSpot(w/o UIS)	96.08	95.23	98.31	96.74
CrisisSpot(w/o CIS)	97.03	96.18	99.21	97.67
CrisisSpot(w/o OF)	96.63	95.75	98.85	97.28
CrisisSpot(U+C+OF)	97.58	96.70	99.80	98.23

'U' represents User Informative Score (UIS)

'C' represents the Crisis Informative Score (CIS)

'OF' represents the Other Features

greater number of crisis-relevant terms, thereby signifying a higher level of informative content related to the crisis.

CrisisSpot (w/o other features): As presented in Table 13, the CrisisSpot (w/o other features) obtains an accuracy of 96.63%, a precision of 95.75%, a recall of 98.85%, and an F1-score of 97.28%. Neglecting to incorporate emotion, sentiment, and user engagement metrics into the model does not accurately capture the emotional context of the content, potentially leading to misinterpretations or oversights in understanding the underlying sentiment. Secondly, the absence of user engagement metrics could hinder the model's ability to gauge the relevance and impact of content, potentially overlooking important interactions. Overall, without considering these features, the model may perform poorly.

CrisisSpot (CIS + UIS + Other Features): This pertains to the suggested model. As indicated in Table 13, our proposed method attains an accuracy of 97.58%, a precision of 96.70%, a recall of 99.80%, and an F1-score of 98.23%. Our proposed approach demonstrates the most favorable outcomes as it integrates all the Social Context Features, contributing to improved crisis content classification.

4.5.6. Model Component Analysis

In Table 14, we illustrate the significance of each module and how they influence the performance of our proposed model. The various variants are CrisisSpot (w/o SCFM), which denotes the proposed model without a Social Contextual Feature Module (SCFM); CrisisSpot (w/o MGLM), which denotes the proposed model without a Multimodal Graph Learning Module (MGLM); CrisisSpot (w/o FEIM), which denotes the proposed model without the feature extraction and interaction module (FEIM); and CrisisSpot (FEIM + MGLM + SCFM) denotes the proposed model.

Table 14
Model Component Comparison for Informative Task

Model	Acc	Prec	Rec	F1
CrisisSpot(w/o SCFM)	94.63	95.86	96.42	96.14
CrisisSpot(w/o MGLM)	93.98	94.20	95.98	94.08
CrisisSpot(w/o FEIM)	95.32	95.44	97.26	96.34
CrisisSpot(SF+ML+FI)	97.58	96.70	99.80	98.23

'w/o' represents without.

'SF' represents the Social Context Feature Module.

'ML' represents the Multimodal Graph Learning Module

'FI' represents the Feature Extraction Interaction Module

CrisisSpot (w/o SCFM): The model that excludes the Social Context Feature module, comprises only two modules: FEIM and MGLM. Within this configuration, we attain an accuracy of 94.63%, a precision of 95.86%, a recall of 96.42%, and an F1-score of 96.14%. Here, both textual and visual features interacted via inverted dual embedded attention, which captures complex patterns as discussed in Section 3.1.3. In MGLM, due to graph knowledge propagation, the features extracted from the multimodal encoder get enriched, hence improving the performance of the model.

CrisisSpot (w/o MGLM): The model without the multimodal graph learning module is denoted as the CrisisSpot (w/o MGLM). In this, we achieve 93.98%, 94.20%, 95.98%, and 94.08% as accuracy, precision, recall, and F1-score. Here,

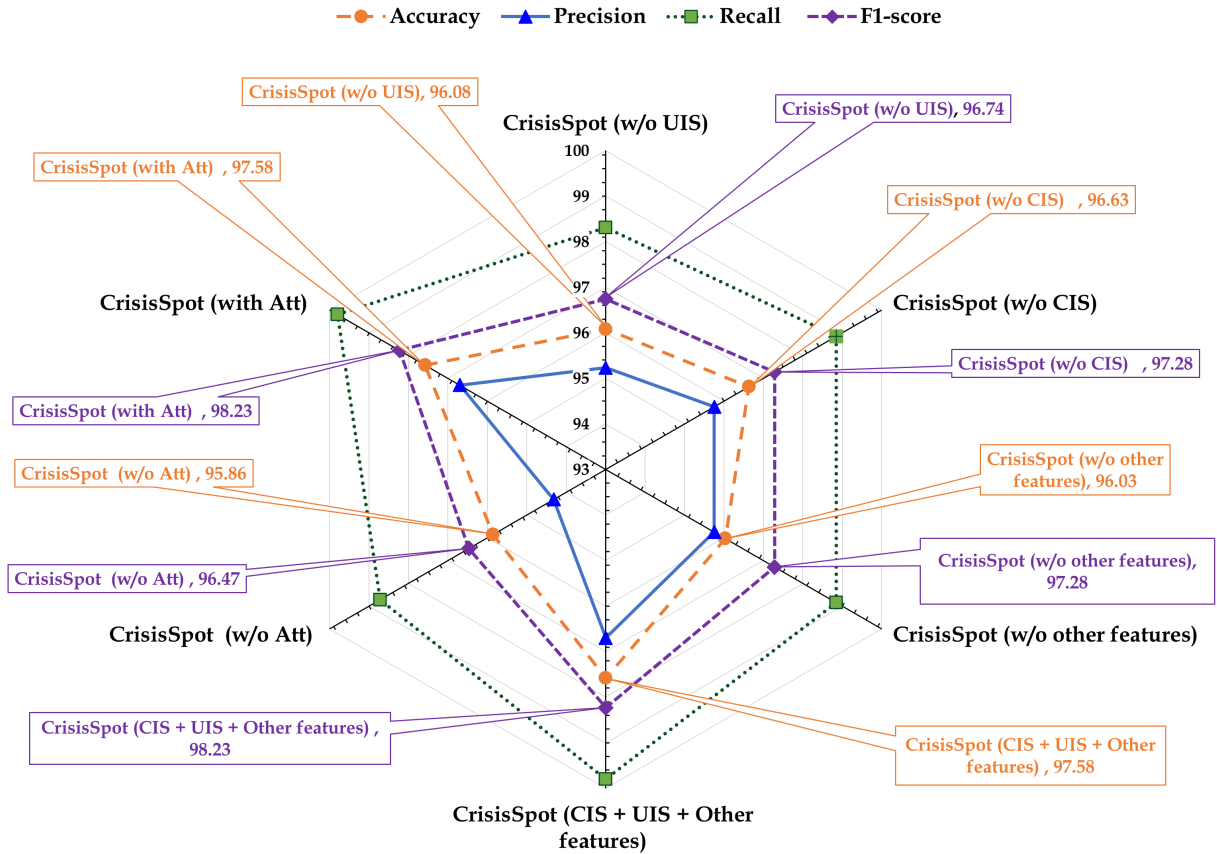


Figure 4: Performance Gain Analysis on Social Context Features and Attention Mechanism

the Social Contextual Features enhance the contextual understanding of the model, and due to the interaction of textual and visual modalities in FEIM, the performance of the model gets enhanced.

CrisisSpot (w/o FEIM): The model that excludes the feature extraction and interaction module is labeled as the CrisisSpot (w/o FEIM). In this configuration, we achieve an accuracy of 95.32%, a precision of 95.44%, a recall of 97.44%, and an F1-score of 97.26%. This model is deprived of the attention mechanism, text features, and visual features, due to the exclusion of the FEIM module. In this model, with the help of multimodal integration of features extracted from the multimodal encoder, text-centric scores, user-centric scores, and graph learning, the model significantly outperforms the other variants.

CrisisSpot (FEIM + MGLM + SCFM): This represents our proposed model, which outperforms all other variations, as shown in Fig. 4. This underscores the efficacy of our proposed approach in comparison to the other variants.

5. Conclusion

In this article, we have introduced an innovative approach for the classification of disaster-related content during emergency situations. Social media platforms have emerged as real-time information sources during disasters; hence, through this article, we highlight both their potential benefits and challenges. By addressing these challenges, our work contributes significantly to disaster response and public safety efforts. Our primary contribution lies in the development of a multimodal attentive learning framework that leverages graph-based and attention-based learning techniques, enhancing the model’s ability to discern complex relationships and subtle nuances within disaster-related content. We have proposed an attention mechanism, Inverted Dual Embedded Attention (IDEA), to capture both

harmonious and contrary information within the content. Our proposed method effectively harnesses multimodal data and Social Context Features to create high-level feature representations, significantly improving model performance. This study concludes that the Crisis Informative Score can be valuable in the identification and categorization of disaster-related content. Furthermore, the research demonstrates that User Informative Score and User Engagement metrics can contribute to assessing the credibility of information shared on social media platforms. Due to the dearth of available training corpus in the disaster domain, we have created a novel multimodal crisis dataset, TSEqD (Turkey-Syria Earthquake Dataset), and annotated for both Informative and Humanitarian Tasks. The novel dataset may prove to be a valuable resource for future research in this domain. Through extensive experiments on two datasets, we demonstrate that CrisisSpot surpasses state-of-the-art benchmarks by substantial margins. In essence, the findings of our work may help researchers build a system for emergency responders and humanitarian organizations utilizing disaster-related social media data.

References

- [1] S. L. Wang, B. Q. Sun, Model of multi-period emergency material allocation for large-scale sudden natural disasters in humanitarian logistics: Efficiency, effectiveness and equity, *International Journal of Disaster Risk Reduction* 85 (2023). doi:10.1016/j.ijdr.2023.103530.
- [2] M. Basu, A. Shandilya, P. Khosla, K. Ghosh, S. Ghosh, Extracting resource needs and availabilities from microblogs for aiding post-disaster relief operations, *IEEE Transactions on Computational Social Systems* 6 (2019). doi:10.1109/TCSS.2019.2914179.
- [3] M. Imran, C. Castillo, F. Diaz, S. Vieweg, Processing social media messages in mass emergency: A survey, *ACM Computing Surveys* 47 (2015). doi:10.1145/2771588.
- [4] L. Li, Q. Zhang, X. Wang, J. Zhang, T. Wang, T. L. Gao, W. Duan, K. K. F. Tsoi, F. Y. Wang, Characterizing the propagation of situational information in social media during covid-19 epidemic: A case study on weibo, *IEEE Transactions on Computational Social Systems* 7 (2020). doi:10.1109/TCSS.2020.2980007.
- [5] F. B. Biggers, S. D. Mohanty, P. Manda, A deep semantic matching approach for identifying relevant messages for social media analysis, *Scientific Reports* 13 (2023). doi:10.1038/s41598-023-38761-y.
- [6] L. Shi, J. Luo, C. Zhu, F. Kou, G. Cheng, X. Liu, A survey on cross-media search based on user intention understanding in social networks, *Information Fusion* 91 (2023). doi:10.1016/j.inffus.2022.11.017.
- [7] T. Baltrusaitis, C. Ahuja, L. P. Morency, Multimodal machine learning: A survey and taxonomy (2019). doi:10.1109/TPAMI.2018.2798607.
- [8] M. Imran, F. Offi, D. Caragea, A. Torralba, Using ai and social media multimodal content for disaster response and management: Opportunities, challenges, and future directions (2020). doi:10.1016/j.ipm.2020.102261.
- [9] Z. Ahmad, R. Jindal, N. S. Mukuntha, A. Ekbal, P. Bhattacharyya, Multi-modality helps in crisis management: An attention-based deep learning approach of leveraging text for image classification, *Expert Systems with Applications* 195 (2022). doi:10.1016/j.eswa.2022.116626.
- [10] S. Madichetty, M. Sridevi, A neural-based approach for detecting the situational information from twitter during disaster, *IEEE Transactions on Computational Social Systems* 8 (2021). doi:10.1109/TCSS.2021.3064299.
- [11] C. Wang, D. Zhao, X. Qi, Z. Liu, Z. Shi, A hierarchical decoder architecture for multilevel fine-grained disaster detection, *IEEE Transactions on Geoscience and Remote Sensing* 61 (2023). doi:10.1109/TGRS.2023.3264811.
- [12] X. Wu, J. Mao, H. Xie, G. Li, Identifying humanitarian information for emergency response by modeling the correlation and independence between text and images, *Information Processing and Management* 59 (2022). doi:10.1016/j.ipm.2022.102977.
- [13] F. Alam, S. Joty, M. Imran, Graph based semi-supervised learning with convolution neural networks to classify crisis related tweets, 12th International AAAI Conference on Web and Social Media, ICWSM 2018 (2018). doi:10.1609/icwsm.v12i1.15047.
- [14] M. Z. U. Rehman, S. Mehta, K. Singh, K. Kaushik, N. Kumar, User-aware multilingual abusive content detection in social media, *Information Processing and Management* 60 (2023). doi:10.1016/j.ipm.2023.103450.
- [15] C. Esposito, A. Galli, V. Moscato, G. Sperlí, Multi-criteria assessment of user trust in social reviewing systems with subjective logic fusion, *Information Fusion* 77 (2022). doi:10.1016/j.inffus.2021.07.012.
- [16] J. Zhang, Z. Yin, P. Chen, S. Nichele, Emotion recognition using multi-modal data and machine learning techniques: A tutorial and review, *Information Fusion* 59 (2020). doi:10.1016/j.inffus.2020.01.011.
- [17] H. Hao, Y. Wang, Leveraging multimodal social media data for rapid disaster damage assessment, *International Journal of Disaster Risk Reduction* 51 (2020). doi:10.1016/j.ijdr.2020.101760.
- [18] M. Abavisani, L. Wu, S. Hu, J. Tetreault, A. Jaimes, Multimodal categorization of crisis events in social media, in: *Proceedings of the IEEE/CVF Conference on Computer Vision and Pattern Recognition*, 2020, pp. 14679–14689. doi:10.1109/CVPR42600.2020.01469.
- [19] W. Gao, L. Li, X. Zhu, Y. Wang, Detecting disaster-related tweets via multimodal adversarial neural network, *IEEE Multimedia* 27 (2020). doi:10.1109/MMUL.2020.3012675.
- [20] A. S. Shirkhorshidi, S. Aghabozorgi, T. Y. Wah, A comparison study on similarity and dissimilarity measures in clustering continuous data, *PLoS ONE* 10 (2015). doi:10.1371/journal.pone.0144059.
- [21] L. Wu, C. J. Hsieh, S. Li, J. Sharpnack, Stochastic shared embeddings: Data-driven regularization of embedding layers, in: *Advances in Neural Information Processing Systems*, Vol. 32, 2019, p. 24–34.
- [22] W. L. Hamilton, R. Ying, J. Leskovec, Inductive representation learning on large graphs, *Advances in Neural Information Processing Systems* 2017-December (2017).

- [23] S. Madichetty, S. M., A novel method for identifying the damage assessment tweets during disaster, *Future Generation Computer Systems* 116 (2021). doi:10.1016/j.future.2020.10.037.
- [24] S. H. Ghafarian, H. S. Yazdi, Identifying crisis-related informative tweets using learning on distributions, *Information Processing and Management* 57 (2020). doi:10.1016/j.ipm.2019.102145.
- [25] K. Rudra, N. Ganguly, P. Goyal, S. Ghosh, Extracting and summarizing situational information from the twitter social media during disasters, *ACM Transactions on the Web* 12 (2018). doi:10.1145/3178541.
- [26] A. Kumar, J. P. Singh, S. Saumya, A comparative analysis of machine learning techniques for disaster-related tweet classification, *IEEE Region 10 Humanitarian Technology Conference, R10-HTC 2019-November* (2019). doi:10.1109/R10-HTC47129.2019.9042443.
- [27] S. Xie, C. Hou, H. Yu, Z. Zhang, X. Luo, N. Zhu, Multi-label disaster text classification via supervised contrastive learning for social media data, *Computers and Electrical Engineering* 104 (2022). doi:10.1016/j.compeleceng.2022.108401.
- [28] E. Weber, D. P. Papadopoulos, A. Lapedriza, F. Ofli, M. Imran, A. Torralba, Incidents1m: A large-scale dataset of images with natural disasters, damage, and incidents, *IEEE Transactions on Pattern Analysis and Machine Intelligence* 45 (2023). doi:10.1109/TPAMI.2022.3191996.
- [29] F. Alam, T. Alam, M. A. Hasan, A. Hasnat, M. Imran, F. Ofli, Medic: a multi-task learning dataset for disaster image classification, *Neural Computing and Applications* 35 (2023). doi:10.1007/s00521-022-07717-0.
- [30] N. Chaudhuri, I. Bose, Exploring the role of deep neural networks for post-disaster decision support, *Decision Support Systems* 130 (2020). doi:10.1016/j.dss.2019.113234.
- [31] D. T. Nguyen, F. Ofli, M. Imran, P. Mitra, Damage assessment from social media imagery data during disasters, *Proceedings of the 2017 IEEE/ACM International Conference on Advances in Social Networks Analysis and Mining, ASONAM 2017* (2017). doi:10.1145/3110025.3110109.
- [32] F. Alam, F. Ofli, M. Imran, T. Alam, U. Qazi, Deep learning benchmarks and datasets for social media image classification for disaster response, *Proceedings of the 2020 IEEE/ACM International Conference on Advances in Social Networks Analysis and Mining, ASONAM 2020* (2020). doi:10.1109/ASONAM49781.2020.9381294.
- [33] M. Agarwal, M. Leekha, R. Sawhney, R. R. Shah, Crisis-dias: Towards multimodal damage analysis - deployment, challenges and assessment, *AAAI 2020 - 34th AAAI Conference on Artificial Intelligence* (2020). doi:10.1609/aaai.v34i01.5369.
- [34] F. Alam, F. Ofli, M. Imran, Crisismmd: Multimodal twitter datasets from natural disasters, *12th International AAAI Conference on Web and Social Media, ICWSM 2018* (2018). doi:10.1609/icwsm.v12i1.14983.
- [35] R. Koshy, S. Elango, Multimodal tweet classification in disaster response systems using transformer-based bidirectional attention model, *Neural Computing and Applications* 35 (2023). doi:10.1007/s00521-022-07790-5.
- [36] S. Madichetty, S. M., S. Madisetty, A roberta based model for identifying the multi-modal informative tweets during disaster, *Multimedia Tools and Applications* (2023). doi:10.1007/s11042-023-14780-9.
- [37] J. Devlin, M. W. Chang, K. Lee, K. Toutanova, Bert: Pre-training of deep bidirectional transformers for language understanding, *NAACL HLT 2019 - 2019 Conference of the North American Chapter of the Association for Computational Linguistics: Human Language Technologies - Proceedings of the Conference 1* (2019).
- [38] P. Luo, X. Wang, W. Shao, Z. Peng, Towards understanding regularization in batch normalization, *7th International Conference on Learning Representations, ICLR 2019* (2019).
- [39] J. Kohler, H. Daneshmand, A. Lucchi, T. Hofmann, M. Zhou, K. Neymeyr, Towards a theoretical understanding of batch normalization, *arXiv* (2018).
- [40] J. Lu, J. Yang, D. Batra, D. Parikh, Hierarchical question-image co-attention for visual question answering, *Advances in Neural Information Processing Systems* (2016) 289–297.
- [41] T. Jiang, J. Wang, Z. Liu, Y. Ling, Fusion-extraction network for multimodal sentiment analysis, *Lecture Notes in Computer Science (including subseries Lecture Notes in Artificial Intelligence and Lecture Notes in Bioinformatics)* 12085 LNAI (2020). doi:10.1007/978-3-030-47436-2_59.
- [42] A. S. Mozafari, H. S. Gomes, W. Leão, C. Gagné, Unsupervised temperature scaling: Post-processing unsupervised calibration of deep models decisions, *arXiv* 1905.00174 (2019).
- [43] G. Hinton, O. Vinyals, J. Dean, Distilling the knowledge in a neural network, *arXiv preprint arXiv:1503.02531* (2015).
- [44] T. Nguyen, F. Pernkopf, M. Kosmider, Acoustic scene classification for mismatched recording devices using heated-up softmax and spectrum correction, in: *ICASSP 2020-2020 IEEE International Conference on Acoustics, Speech and Signal Processing (ICASSP), IEEE, 2020*, pp. 126–130.
- [45] A. Vaswani, N. Shazeer, N. Parmar, J. Uszkoreit, L. Jones, A. N. Gomez, Łukasz Kaiser, I. Polosukhin, Attention is all you need, in: *Advances in Neural Information Processing Systems*, Vol. 30, 2017, pp. 6000–6010.
- [46] P. Shaw, J. Uszkoreit, A. Vaswani, Self-attention with relative position representations, in: *Proceedings of the 2018 Conference of the North American Chapter of the Association for Computational Linguistics: Human Language Technologies, Volume 2 (Short Papers), Vol. 2, 2018*, pp. 464–468. doi:10.18653/v1/n18-2074.
- [47] A. Radford, J. W. Kim, C. Hallacy, A. Ramesh, G. Goh, S. Agarwal, G. Sastry, A. Askell, P. Mishkin, J. Clark, G. Krueger, I. Sutskever, Learning transferable visual models from natural language supervision, *Proceedings of Machine Learning Research* 139 (2021).
- [48] C. J. Hutto, E. Gilbert, Vader: A parsimonious rule-based model for sentiment analysis of social media text, *Proceedings of the 8th International Conference on Weblogs and Social Media, ICWSM 2014* (2014). doi:10.1609/icwsm.v8i1.14550.
- [49] S. M. Mohammad, P. D. Turney, Crowdsourcing a word-emotion association lexicon, *Computational Intelligence* 29 (2013). doi:10.1111/j.1467-8640.2012.00460.x.
- [50] A. Olteanu, C. Castillo, F. Diaz, S. Vieweg, Crisislex: A lexicon for collecting and filtering microblogged communications in crises, *Proceedings of the 8th International Conference on Weblogs and Social Media, ICWSM 2014* (2014). doi:10.1609/icwsm.v8i1.14538.
- [51] K. He, X. Zhang, S. Ren, J. Sun, Deep residual learning for image recognition, *Proceedings of the IEEE Computer Society Conference on Computer Vision and Pattern Recognition 2016-December* (2016). doi:10.1109/CVPR.2016.90.

- [52] L. H. Li, M. Yatskar, D. Yin, C.-J. Hsieh, K.-W. Chang, Visualbert: A simple and performant baseline for vision and language, arXiv e-prints (2019) arXiv-1908.
- [53] J. Lu, D. Batra, D. Parikh, S. Lee, Vilbert: Pretraining task-agnostic visiolinguistic representations for vision-and-language tasks, in: Proceedings of the 33rd International Conference on Neural Information Processing Systems, 2019, pp. 13–23.
- [54] W. Kim, B. Son, I. Kim, Vilt: Vision-and-language transformer without convolution or region supervision, in: International Conference on Machine Learning, Vol. 139, PMLR, 2021, pp. 5583–5594.
- [55] A. Khattar, S. M. Quadri, Camm: Cross-attention multimodal classification of disaster-related tweets, IEEE Access 10 (2022). doi:10.1109/ACCESS.2022.3202976.
- [56] I. Sirbu, T. Sosea, C. Caragea, D. Caragea, T. Rebedea, Multimodal semi-supervised learning for disaster tweet classification, in: Proceedings of the 29th International Conference on Computational Linguistics, Vol. 29, 2022, pp. 2711–2723.
- [57] J. H. Yoon, G. H. Choi, C. Choi, Multimedia analysis of robustly optimized multimodal transformer based on vision and language co-learning, Information Fusion 100 (2023). doi:10.1016/j.inffus.2023.101922.
- [58] M. Rezk, N. Elmadany, R. K. Hamad, E. F. Badran, Categorizing crises from social media feeds via multimodal channel attention, IEEE Access 11 (2023). doi:10.1109/ACCESS.2023.3294474.
- [59] O. Susladkar, G. Deshmukh, D. Makwana, S. Mittal, R. S. C. Teja, R. Singhal, Gafnet: A global fourier self attention based novel network for multi-modal downstream tasks, Proceedings - 2023 IEEE Winter Conference on Applications of Computer Vision, WACV 2023 (2023). doi:10.1109/WACV56688.2023.00521.
- [60] T. Liang, G. Lin, M. Wan, T. Li, G. Ma, F. Lv, Expanding large pre-trained unimodal models with multimodal information injection for image-text multimodal classification, Proceedings of the IEEE Computer Society Conference on Computer Vision and Pattern Recognition 2022-June (2022). doi:10.1109/CVPR52688.2022.01505.